Supporting information

Synthesis and Structure Elucidation of Triarylmethyl Radicals with Anthryl Substitution

Peng Wang,[ab] Jinlian Hu,[a] Zhuofan Xu,[a] Zhaofangzhou Pu,[a] Sota Sato,[c] Xiaotao Zhang*[d], Wenping Hu*[be], Zhe Sun*[abe]

[a]*Institute of Molecular Plus, Department of Chemistry, Tianjin University, 92 Weijin Road, Tianjin, 300072 China*

[b]*Tianjin Key Laboratory of Molecular Optoelectronic Sciences, Department of Chemistry, School of Science, Tianjin University, Tianjin 300072 China*

[c]*Department of Applied Chemistry, Integrated Molecular Structure Analysis Laboratory, Social Cooperation Program, The University of Tokyo, Hongo, Bunkyo-ku, Tokyo 113-8656 Japan*

[d]*Institute of Molecular Aggregation Science, Tianjin University, Tianjin 300072 China*

[e]*Haihe Laboratory of Sustainable Chemical Transformations, Tianjin 300192 China*

Table of Contents

1. Experimental section and synthesis

1.1 General information

Most reagents were purchased from commercial sources and used without further purification, unless otherwise stated. Anhydrous tetrahydrofuran (THF) and toluene were distilled with sodium. Dichloromethane (DCM) was dried over CaH_2 and distilled prior to use. All reactions dealing with moisture-sensitive compounds were performed by standard Schlenk techniques in oven-dried reaction vessels under argon atmosphere. Column chromatography was performed with silica gel (200-300 mesh). ^1H NMR and ^{13}C NMR spectra were recorded on JNM-ECZ600R/S1 and Bruker-AVANCE III instrument calibrated using residual solvent as an internal reference ($CHCl_3$: δ 7.26 ppm for ^1H, δ 77.16 ppm for ^{13}C; CH_2Cl_2: δ 5.32 ppm for ^1H; toluene: δ 7.09, 7.01 and 6.97 ppm for ^1H; trifluoroacetic acid (TFA): δ 11.50 ppm for ^1H). The variable-temperature NMR (VT-NMR) measurements were performed in degassed CD_2Cl_2. The following abbreviations were used to explain multiplicities: s = singlet, d = doublet, t = triplet, dd = doublet of doublets, dt = doublet of triplets, m = multiplet, br = broad. High resolution Electrospray Ionization (ESI) mass spectra were recorded on Bruker MicroTOF-Q II instrument. Analytical high-pressure liquid chromatography (HPLC) was performed with SHIMADZU LC-2030C 3D Plus instrument. UV-vis-NIR spectra were recorded on SHIMADZU UV-2600 spectrophotometer in DCM. The diffraction data of **7b** (at 100 K), **8a** (at 293 K) and **8b** (at 160 K) were collected on XtaLAB Synergy diffractometer equipped with Hypix6000HE detector using Cu Kα radiation (λ = 1.54184 Å). The electrochemical measurements were carried out in dry DCM or THF containing n-Bu_4NPF_6 as supporting electrolyte under argon atmosphere by CHI 620E electrochemical analyzer. A three-electrode system consisting of glassy carbon as working electrode, Pt as counter electrode and $Ag/AgNO_3$ as reference electrode was applied for data collection of cyclic voltammetry (CV) curves and differential pulse voltammetry (DPV) curves. The potential was calibrated against ferrocene/ferrocenium couple. The oxidation titration was performed by adding dry acetonitrile solution of $NOSbF_6$ into dry DCM solution of **8a** and **8b**. The electron spin resonance (ESR) spectra were recorded on JES-FA200 spectrometer. The hyperfine constant was fitted using the Easyspin package in Matlab.[1] The melting point were recorded on RY-IG melting point detector. Thermogravimetric analysis (TGA) was carried out on a METTLER TOLEDO TGA2 apparatus with a scanning rate of 10 ºC /min. Susceptibility data for **8a** powder was recorded on Quantum Design MPMS 3 SQUID magnetometer in the temperature range of 2 K-380 K with an applied magnetic field of 0.8 T.

1.2 Synthesis

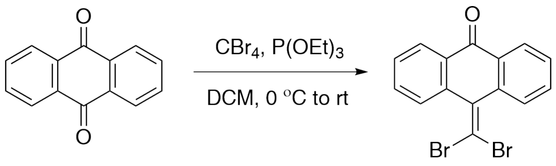

1a 51% 2a

2a: Compound **1a** (3.12 g, 15.0 mmol) and CBr$_4$ (5.97 g, 18.0 mmol) were added to a 500 mL round-bottom-flask equipped with a magnetic stirring bar. Then the flask was evacuated and refilled with argon for three times, DCM (300.0 mL) was added and the mixture was stirred for at 0 ºC for 5 minutes. Then P(OEt)$_3$ (6.04 mL, 36.0 mmol) was added dropwise and the solution was warmed up to room temperature and stirred for 18 hours. Subsequently, the reaction mixture was concentrated under vacuum and the residue was directly purified by column chromatography on silica gel (petroleum ether (PE):toluene = 20:1 to 10:1) to give the desired product **2a** (2.78 g, 51% yield) as a white solid[2]. ^{1}H NMR (600 MHz, CDCl$_3$) δ ppm 8.10 – 8.07 (m, 4H), 7.56 – 7.54 (m, 2H), 7.49 (t, *J* = 7.5 Hz, 2H). ^{13}C NMR (150 MHz, CDCl$_3$) δ ppm 185.32, 138.25, 136.69, 132.53, 131.10, 128.86, 128.61, 126.77, 93.74. HRMS (ESI) *m*/*z* [M + Na]$^+$ calcd for $C_{15}H_8Br_2ONa^+$ 384.8834, found 384.8838.

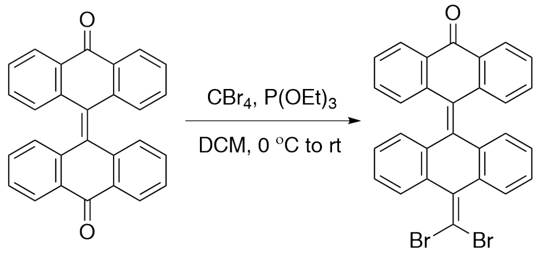

1b 53% 2b

2b: Compound **1b** (1.15 g, 3.0 mmol) and CBr$_4$ (1.29 g, 3.9 mmol) were added to a 250 mL round-bottom-flask equipped with a magnetic stirring bar. Then the flask was evacuated and refilled with argon for three times. DCM (120.0 mL) was added and the mixture was stirred at 0 ºC for 5 minutes. Then P(OEt)$_3$ (1.30 mL, 7.8 mmol) was added dropwise and the solution was warmed up to room temperature and stirred for 24 hours. Subsequently, the reaction mixture was concentrated under vacuum and the residue was directly purified by column chromatography on silica gel (PE:DCM = 5:1 to 1:1) to give the desired product **2a** (849.7 mg, 53% yield) as a yellow solid. ^{1}H NMR (600 MHz, CDCl$_3$) δ ppm 8.14 (dd, *J* = 7.7, 1.1 Hz, 2H), 7.89 – 7.88 (m, 2H), 7.40 (dt, *J* = 7.7, 1.1 Hz, 2H), 7.28 (d, *J* = 7.4 Hz, 2H), 7.23 – 7.20 (m, 4H), 6.95 (dt, *J* = 7.6, 1.1 Hz, 2H), 6.89 – 6.88 (m, 2H). ^{13}C NMR (150 MHz, CDCl$_3$) δ ppm 186.63, 140.81, 138.80, 137.97, 137.09, 135.99, 134.05, 130.28, 130.11, 128.57, 128.29, 128.15, 128.02, 126.79, 126.70, 126.69, 89.73. HRMS (ESI) *m*/*z* [M + Na]$^+$ calcd for $C_{29}H_{16}Br_2ONa^+$ 562.9442, found 562.9440.

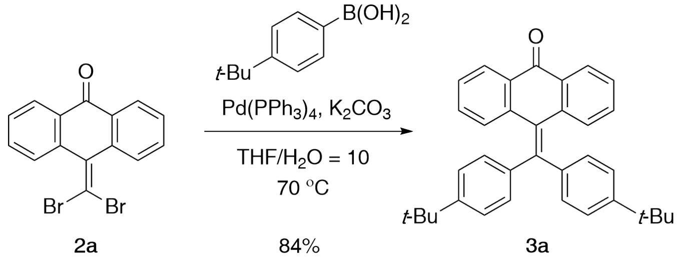

3a: Compound **2a** (361.9 mg, 1.0 mmol), 4-*tert*-butylphenylboronic acid (623.1 mg, 3.5 mmol), K_2CO_3 (691.0 mg, 5.0 mmol) and $Pd(PPh_3)_4$ (115.6 mg, 0.1 mmol) were added to a 100 mL Schlenk tube equipped with a magnetic stirring bar. Then the tube was evacuated and refilled with argon for three times before degassed THF (50.0 mL) and H_2O (5.0 mL) were added. The solution was heated to 70 ºC and stirred for 12 hours. After cooling to room temperature, the mixture was filtered through a thin celite pad with ethyl acetate as eluent. The filtrate was washed with water, brine, and dried over Na_2SO_4. After filtration and concentration under vacuum, the residue was purified by column chromatography on silica gel (PE:EtOAc = 20:1) to give the desired product **3a** (396.6 mg, 84% yield) as a white solid. ^{1}H NMR (600 MHz, CD_2Cl_2) δ ppm 8.06 (d, *J* = 7.8 Hz, 2H), 7.28 – 7.26 (m, 6H), 7.15 – 7.15 (m, 6H), 7.05 (t, *J* = 7.6 Hz, 2H), 1.26 (s, 18H). ^{13}C NMR (150 MHz, CD_2Cl_2) δ ppm 185.96, 150.59, 146.83, 140.80, 139.95, 133.31, 130.65, 130.58, 128.79, 127.36, 126.40, 125.83, 34.76, 31.38. HRMS (ESI) *m/z* $[M + H]^+$ calcd for $C_{35}H_{35}O^+$ 471.2682, found 471.2694.

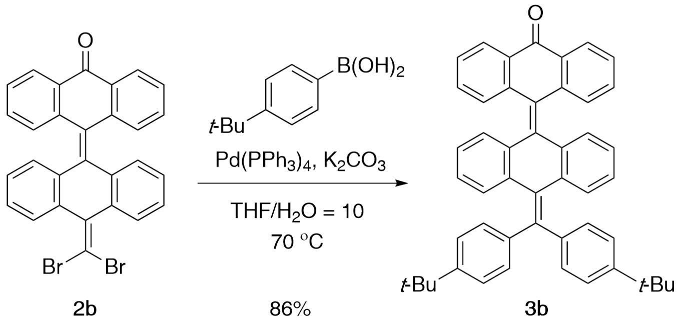

3b: Compound **3b** was synthesized from compound **2b** by applying the same procedure for the synthesis of **2a** described above. With 1.5 mmol (806.9 mg) of compound **2b**, compound **3b** was obtained as a yellow solid (838.0 mg, 86%). ^{1}H NMR (600 MHz, $CDCl_3$) δ ppm 8.18 (dd, *J* = 7.7, 1.1 Hz, 2H), 7.44 – 7.40 (m, 6H), 7.37 – 7.37 (m, 6H), 7.29 – 7.26 (m, 2H), 7.08 – 7.07 (m, 2H), 6.88 (dd, *J* = 7.6, 0.9 Hz, 2H), 6.84 (dt, *J* = 7.6, 1.3 Hz, 2H), 6.78 (dt, *J* = 7.5, 1.2 Hz, 2H), 1.33 (s, 18H). ^{13}C NMR (150 MHz, $CDCl_3$) δ ppm 186.81, 149.81, 140.64, 139.41, 139.37, 139.34, 138.04, 137.67, 134.84, 134.12, 130.18, 129.95, 129.26, 128.98, 128.00, 127.80, 126.84, 126.72, 126.28, 125.32, 124.99, 34.65, 31.51. HRMS (ESI) *m/z* $[M + H]^+$ calcd for $C_{49}H_{43}O^+$ 647.3308, found 647.3307.

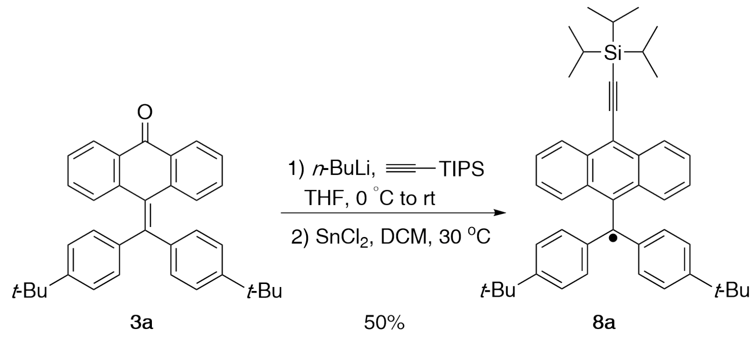

8a: An over-dried 250 mL two-neck round-bottom-flask equipped with a magnetic stirring bar was evacuated and refilled with argon for three times. Triisopropylsilylacetylene (1.64 g, 9.0 mmol) and 60 mL anhydrous THF were added successively, then the solution was cooled to 0 °C by ice bath. *n*-BuLi in hexane (1.6 M, 5.63 mL, 9.0 mmol) was added dropwise at 0 °C. The reaction mixture was stirred for 1 hour at 0 °C, and a solution of compound **3a** (2.12 g, 4.5 mmol) in THF (30.0 mL) was added dropwise. The reaction mixture was warmed to room temperature and stirred for 3 hours. Then the mixture was quenched with H_2O and concentrated under vacuum. The residue was redissolved in DCM, washed with water and dried over Na_2SO_4. After filtration and concentration under vacuum, the crude product was obtained as a colorless solid and was used in the next step directly.

The crude product was added to a 100 mL round-bottom-flask equipped with a magnetic stirring bar. The flask was evacuated and refilled with argon for three times before degassed DCM (60.0 mL) was added. Then $SnCl_2$ (4.26 g, 22.5 mmol) was added and stirred for 2 hours at 30 °C. The mixture was filtered and concentrated under vacuum, and the crude material was redissolved in degassed toluene and filtered with membrane filter (pore size 0.4 μm) and recrystallized in degassed 1:1 mixture of toluene and methanol to give **8a** (1.44 g, 50% yield) as a purple solid. HRMS (ESI) *m/z* $[M]^+$ calcd for $C_{46}H_{55}Si^{\bullet}$ 635.4068, found 635.4056.

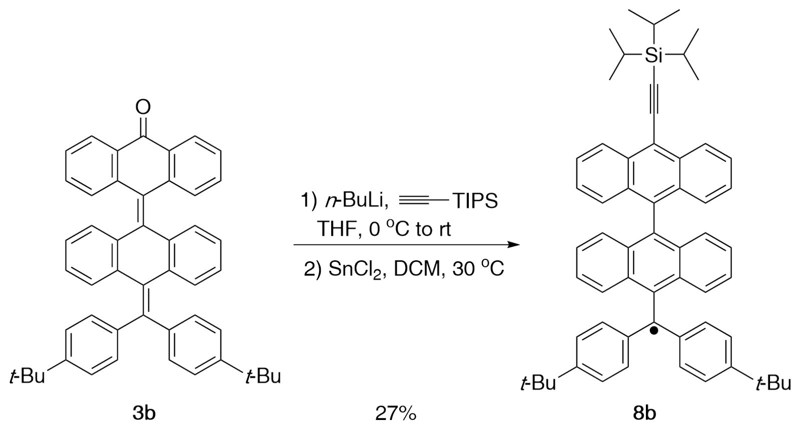

8b: An over-dried 250 mL two-neck round-bottom-flask equipped with a magnetic stirring bar was evacuated and refilled with argon for three times. Triisopropylsilylacetylene (1.28 g, 7.0 mmol) and 60 mL anhydrous THF were added successively, then the solution was cooled to 0 ºC by ice bath. *n*-BuLi in hexane (1.6 M, 4.38 mL, 7.0 mmol) was added dropwise at 0 ºC. The reaction mixture was stirred for 1 hour at 0 ºC, and a solution of compound **3b** (2.26 g, 3.5 mmol) in THF (30.0 mL) was added dropwise. The reaction mixture was warmed to room temperature and stirred for 1 hour. Then the mixture was quenched with H_2O and concentrated under vacuum. The residue was redissolved in DCM, washed with water and dried over Na_2SO_4. After filtration and concentration under vacuum, the crude product was obtained as a colorless solid and was used in the next step directly.

The crude product was added to a 100 mL round-bottom-flask equipped with a magnetic stirring bar. The flask was evacuated and refilled with argon for three times before degassed DCM (60.0 mL) was added. Then $SnCl_2$ (3.32 g, 17.5 mmol) was added and stirred for 10 hours at 30 ºC. The mixture was filtered and concentrated under vacuum, and the crude material was redissolved in degassed toluene and filtered with membrane filter (pore size 0.4 μm) and recrystallized in degassed 1:1 mixture of toluene and isopropanol to give **8b** (0.75 g, 27% yield) as a red solid. HRMS (ESI) *m*/*z* $[M]^+$ calcd for $C_{60}H_{63}Si^{\bullet}$ 811.4694, found 811.4686.

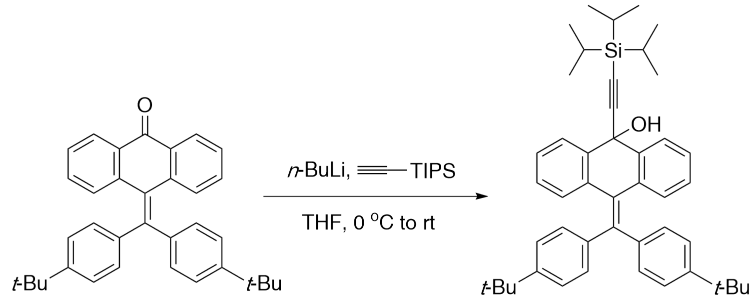

3a 4a

4a: Compound **4a** was synthesized from compound **3a** by applying the same procedure for the synthesis of **8a** described above. With 0.3 mmol (141.1 mg) of **3a**, crude compound **4a** was obtained. After purification using flash column chromatography on silica gel (PE to PE:EtOAc = 30:1), compound **4a** (190.9 mg, 98% yield) was obtained as a colorless solid. ^1H NMR (600 MHz, $CDCl_3$) δ ppm 8.00 (d, *J* = 7.5 Hz, 2H), 7.28 (d, *J* = 8.3 Hz, 4H), 7.21 (d, *J* = 8.3 Hz, 4H), 7.16 – 7.13 (m, 2H), 6.98 (d, *J* = 7.7 Hz, 2H), 6.89 – 6.87 (m, 2H), 2.84 (s, 1H), 1.26 (s, 18H), 1.15 (m, 21H). ^{13}C NMR spectrum was not obtained as **4a** quickly decomposes in $CDCl_3$. HRMS (ESI) *m*/*z* $[M + Na]^+$ calcd for $C_{46}H_{56}OSiNa^+$ 675.3993, found 675.3996.

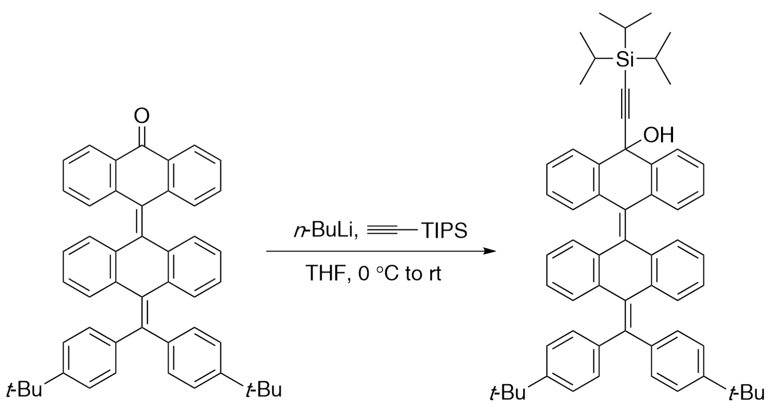

3b 95% **4b**

4b: Compound **4b** was synthesized from compound **3b** by applying the same procedure for the synthesis of **8b** described above. With 0.2 mmol (129.3 mg) of **3b**, crude compound **4b** was obtained. After purification using column chromatography on silica gel (PE to PE:DCM = 1:1), compound **4b** (161.5 mg, 95% yield) was obtained as a colorless solid. ^{1}H NMR (400 MHz, $CDCl_3$) δ ppm 7.92 (d, J = 7.4 Hz, 2H), 7.41 (d, J = 8.4 Hz, 4H), 7.34 – 7.28 (m, 6H), 7.21 (d, J = 7.2 Hz, 2H), 7.10 – 7.06 (m, 2H), 7.05 – 7.01 (m, 4H), 6.81 – 6.76 (m, 2H), 6.72 (td, J = 7.5, 1.1 Hz, 2H), 3.07 (s, 1H), 1.32 (s, 18H), 0.88 – 0.88 (m, 21H). ^{13}C NMR (100 MHz, $CDCl_3$) δ ppm 149.61, 142.88, 140.17, 139.79, 138.93, 137.42, 135.66, 135.16, 133.34, 130.13, 129.42, 129.18, 128.61, 128.51, 127.16, 126.28, 125.71, 125.25, 124.50, 122.47, 108.86, 83.94, 68.99, 34.65, 31.55, 18.69, 11.25. HRMS (ESI) m/z $[M + Na]^+$ calcd for $C_{60}H_{64}OSiNa^+$ 851.4619, found 851.4615.

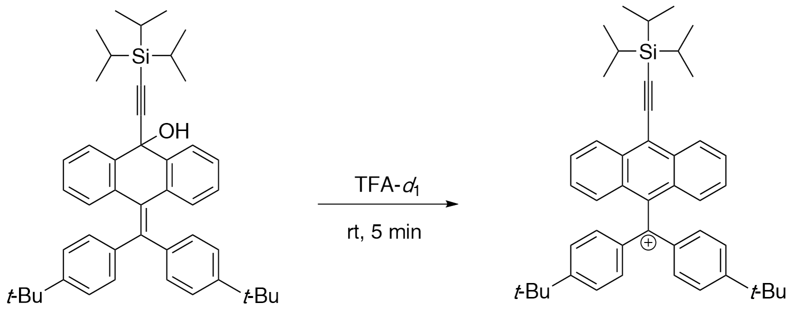

4a **6a**

6a: Compound **4a** (15.0 mg) was placed in an NMR tube and TFA-d_1 (0.6 mL) was added at room temperature, generating a deep yellow solution of **6a**. ^{1}H NMR (400 MHz, TFA-d_1) δ ppm 8.94 (d, J = 8.7 Hz, 2H), 7.82 (br, 4H), 7.68 (br, 4H), 7.63 – 7.60 (m, 2H), 7.42 – 7.38 (m, 2H), 7.33 (d, J = 8.9 Hz, 2H), 1.44 (s, 18H), 1.35 – 1.33 (m, 21H). ^{13}C NMR (100 MHz, TFA-d_1) δ ppm 203.05, 173.78, 143.85, 142.53, 138.66, 138.07, 135.74, 134.50, 133.32, 132.68, 130.68, 130.52, 129.78, 128.70, 104.44, 38.70, 31.36, 19.61, 13.49.

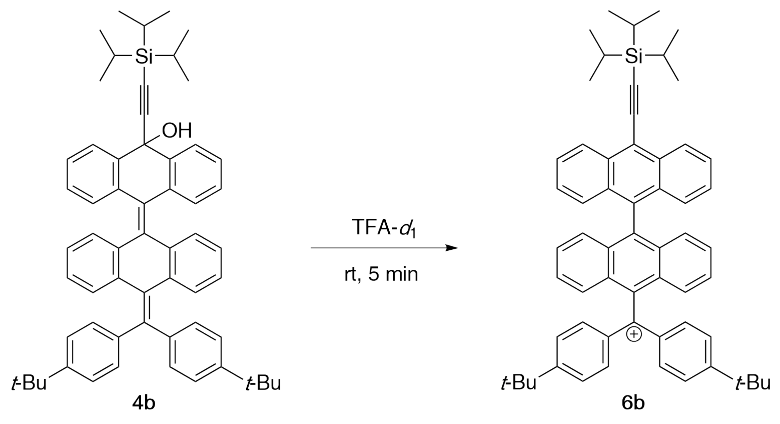

6b: Compound **4b** (15.0 mg) was placed in an NMR tube and TFA-d_1 (0.6 mL) was added at room temperature, generating a deep yellow solution of **6b**. ^{1}H NMR (600 MHz, TFA-d_1) δ ppm 8.91 (d, *J* = 8.8 Hz, 2H), 7.76 (br, 8H), 7.48 – 7.45 (m, 2H), 7.37 (d, *J* = 8.9 Hz, 2H), 7.30 – 7.26 (m, 2H), 7.24 (d, *J* = 8.8 Hz, 2H), 7.07 – 7.01 (m, 6H), 1.39 (s, 18H), 1.32 – 1.31 (m, 21H). ^{13}C NMR spectrum was not obtained as **6b** gradually decomposed in TFA-d_1.

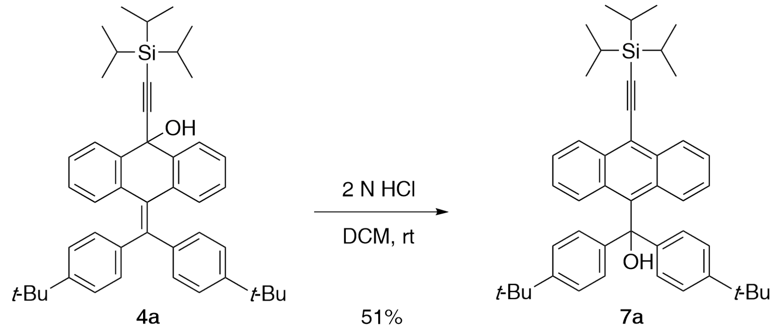

7a: **4a** (193.0 mg, 0.30 mmol) was added to a 100 mL round-bottom-flask equipped with a magnetic stirring bar. Then DCM (50.0 mL) and 2 N HCl solution were added and the solution was stirred at room temperature for 3 days. Then the mixture was washed with water and dried over Na_2SO_4. After filtration and concentration under vacuum, the residue was purified by column chromatography on silica gel (PE:EtOAc = 20:1) to give compound **7a** (99.0 mg, 51% yield) as a yellow solid. ^{1}H NMR (400 MHz, $CDCl_3$) δ ppm 8.67 (d, *J* = 8.5 Hz, 2H), 7.92 (d, *J* = 9.2 Hz, 2H), 7.41 – 7.37 (m, 2H), 7.30 (d, *J* = 8.6 Hz, 4H), 7.20 (d, *J* = 8.5 Hz, 4H), 7.06 – 7.02 (m, 2H), 3.00 (s, 1H), 1.31 (s, 18H), 1.28 – 1.27 (m, 21H). ^{13}C NMR (100 MHz, $CDCl_3$) δ ppm 150.60, 145.42, 141.28, 133.39, 130.47, 128.77, 127.53, 127.08, 125.57, 125.42, 123.87, 119.59, 103.92, 103.82, 83.95, 34.64, 31.48, 19.05, 11.66. HRMS (ESI) *m*/*z* [M + Na]$^+$ calcd for $C_{46}H_{56}OSiNa^+$ 675.3993, found 675.3993.

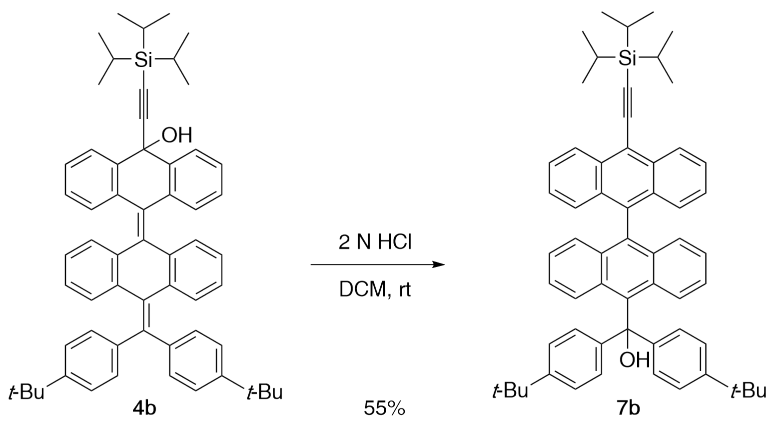

7b: **4b** (16.5 mg, 0.02 mmol) was added to a 100 mL round-bottom-flask equipped with a magnetic stirring bar. Then DCM (20.0 mL) and 2 N HCl solution (0.2 mL) were added and the solution was stirred at room temperature for 55 hours. The mixture was washed with water and dried over Na_2SO_4. After filtration and concentration under vacuum, the residue was purified by preparative TLC (PE:DCM = 1:1) to give compound **7b** (9.0 mg, 55% yield) as a yellow solid. Melting point: 276–278 ºC; ^{1}H NMR (400 MHz, $CDCl_3$) δ ppm 8.80 (d, *J* = 8.7 Hz, 2H), 8.07 (d, *J* = 9.0 Hz, 2H), 7.59 – 7.55 (m, 2H), 7.42 – 7.37 (m, 8H), 7.25 – 7.21 (m, 2H), 7.16 (d, *J* = 8.7 Hz, 2H), 7.05 (d, *J* = 8.5 Hz, 2H), 7.01 – 6.92 (m, 4H), 3.23 (s, 1H), 1.35 (s, 18H), 1.34 – 1.33 (m, 21H). ^{13}C NMR (100 MHz, $CDCl_3$) δ ppm 150.63, 145.77, 140.70, 135.48, 134.54, 132.94, 131.93, 131.37, 130.55, 128.67, 127.66, 127.62, 127.25, 127.16, 126.83, 126.27, 125.58, 124.80, 123.63, 118.47, 103.67, 103.60, 84.15, 34.70, 31.53, 19.11, 11.71. HRMS (ESI) *m*/*z* $[M + H]^+$ calcd for $C_{60}H_{65}OSi^+$ 829.4799, found 829.4781.

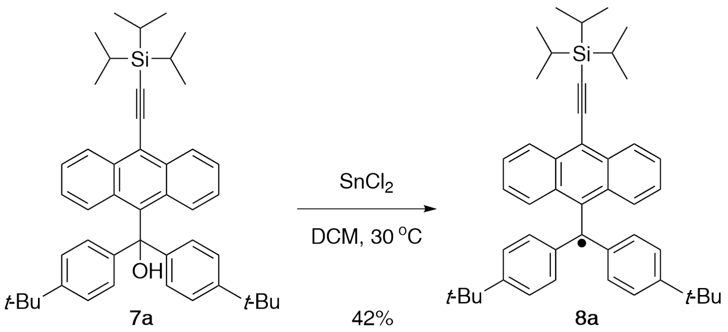

8a: **7a** (48.9 mg, 0.075 mmol) and $SnCl_2$ (71.1 mg, 0.375 mmol) were added to a 25 mL Schlenk tube equipped with a magnetic stirring bar. Then the tube was evacuated and refilled with argon for three times. Degassed DCM (2.0 mL) was added and the solution was stirred at 30 ºC for 4 hours. Then the mixture was filtered and concentrated under vacuum. The crude material was redissolved in degassed toluene and filtered with membrane filter (pore size 0.4 μm) and recrystallized in degassed mixture of toluene and methanol to give **8a** (19.8 mg, 42% yield) as a purple solid. Melting point: 230–232 ºC.

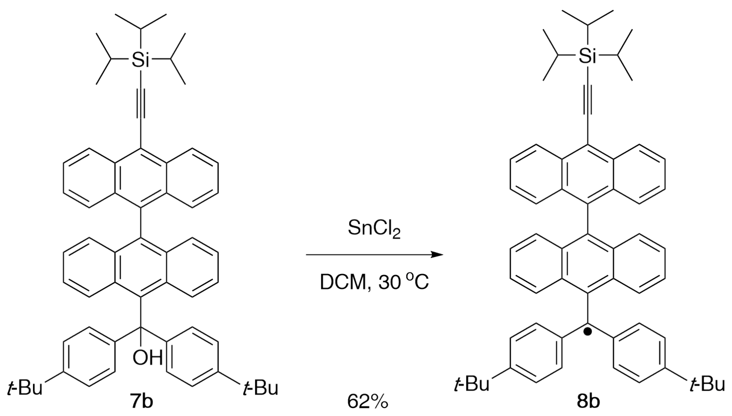

8b: **7b** (49.7 mg, 0.06 mmol) and $SnCl_2$ (56.9 mg, 0.30 mmol) were added to a 25 mL Schlenk tube equipped with a magnetic stirring bar. Then the tube was evacuated and refilled with argon for three times. Degassed DCM (2.0 mL) was added and the solution was stirred at 30 °C for 4 hours. Then the mixture was filtered and concentrated under vacuum. The crude material was redissolved in degassed toluene and filtered with membrane filter (pore size 0.4 μm) and recrystallized in degassed mixture of toluene and isopropanol to give **8b** (30.1 mg, 62% yield) as a red solid. Melting point: 288–290 °C.

Decomposition of **8a** and **8b**

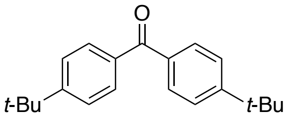

9

8a or **8b** was dissolved in DCM and kept at room temperature in air. After the color of the solution turned into yellow, the solvent was removed and the crude material was purified by column chromatography on silica gel (PE: DCM = 5:1 to DCM). In both cases, compound **9** can be isolated as a light yellow solid. ^{1}H NMR (400 MHz, $CDCl_3$) δ ppm 7.77 (d, J = 8.6 Hz, 4H), 7.49 (d, J = 8.5 Hz, 4H), 1.37 (s, 18H). ^{13}C NMR (100 MHz, $CDCl_3$) δ ppm 196.34, 156.02, 135.25, 130.19, 125.30, 35.23, 31.30. The NMR spectra matched the literature reported data.[3] The formation of **9** may be from the first homolytic cleavage of the elongated C_1-C_2 bond (see crystal structure), followed by the oxidation of the resulted bis(4-(*tert*-butyl)phenyl)methanide.

2. Additional physical data

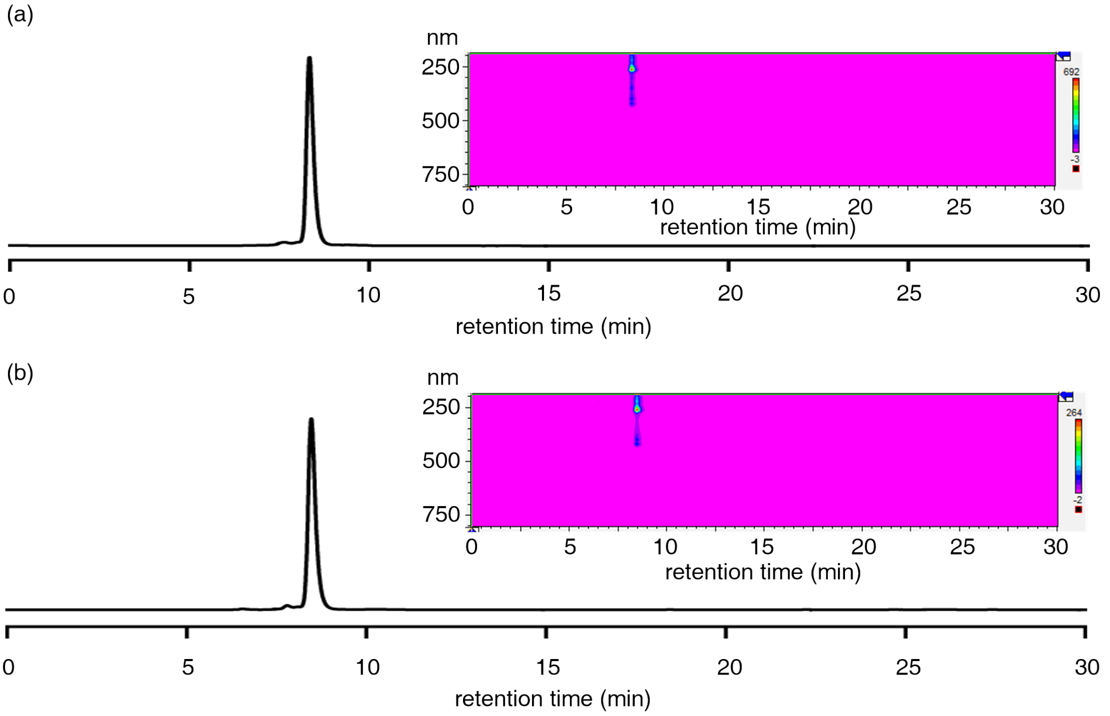

Figure S1. HPLC charts for (a) **8a** and (b) **8b** with Cosmosil 5C18-MS-II column. Chromatographic conditions: flow rate = 0.5 mL/min, eluent = 50% CH_2Cl_2/methanol, column temperature = 25 ºC, detection = 254 nm. Inset: 2D-HPLC chromatograms.

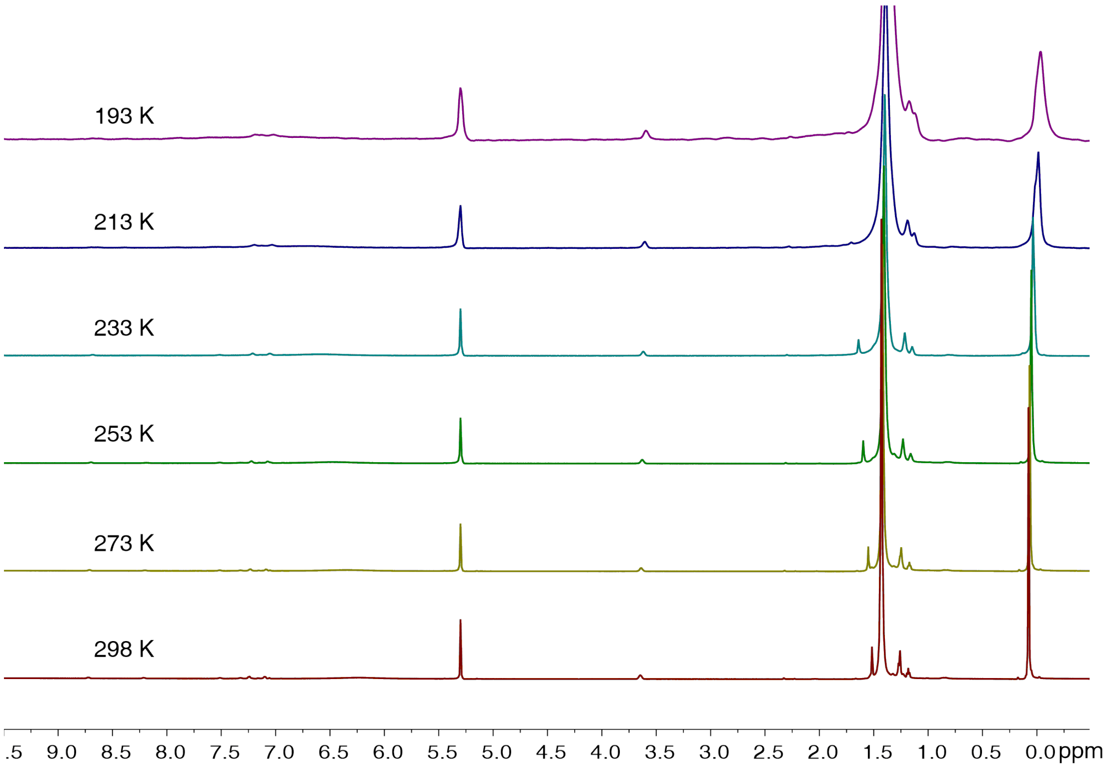

Figure S2. VT-NMR spectra of **8a** in CD_2Cl_2 (600 MHz).

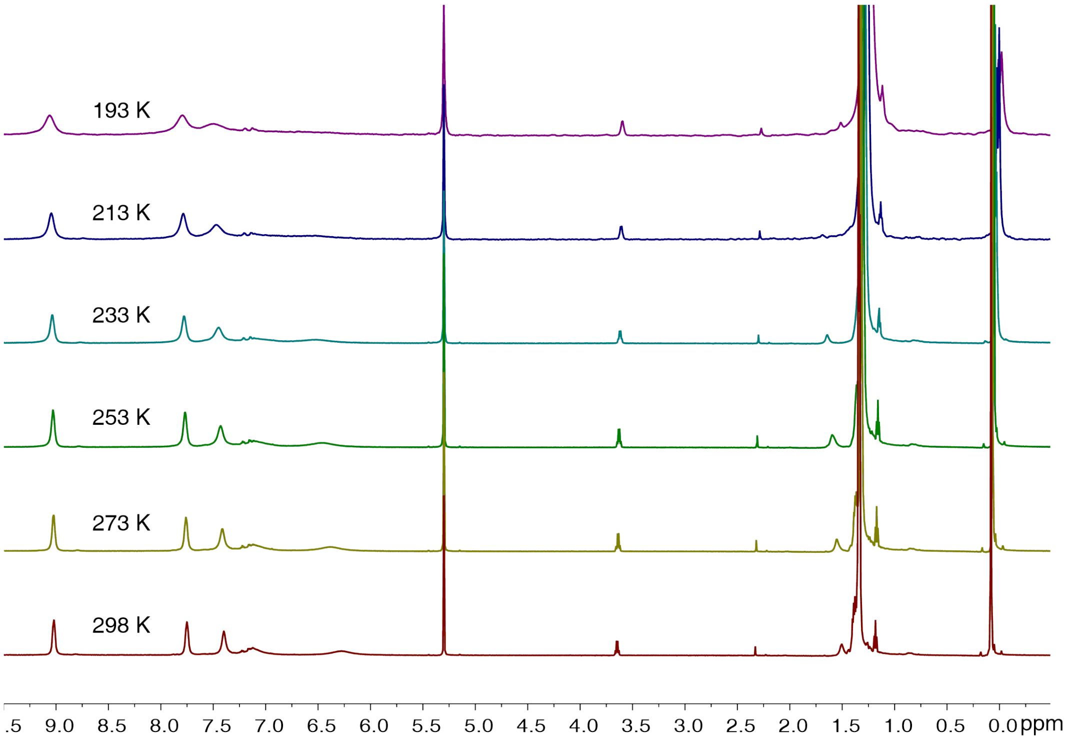

Figure S3. VT-NMR spectra of **8b** in CD_2Cl_2 (600 MHz).

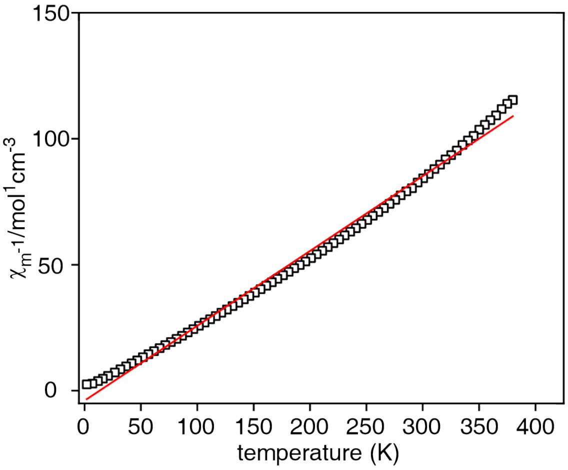

Figure S4. Inverse susceptibility of **8a** versus temperature based on Curie law.

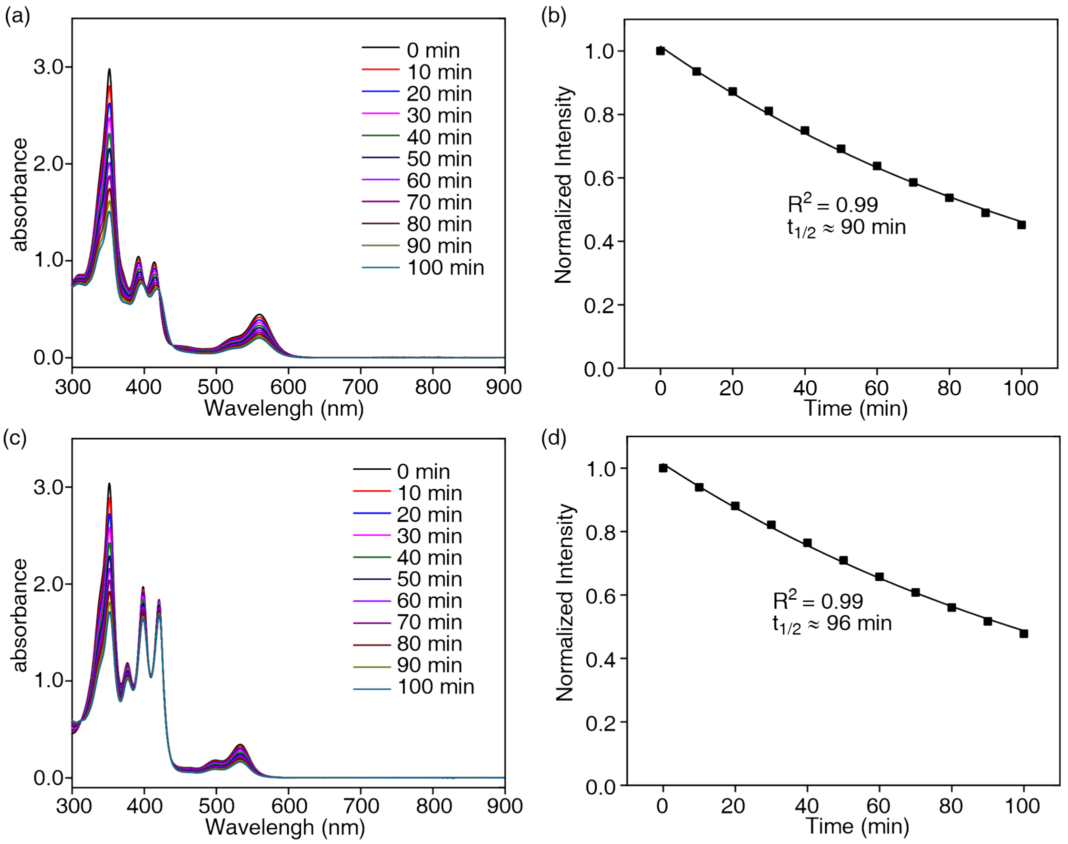

Figure S5. The UV-*vis* absorption spectral changes of **8a** (a) and **8b** (c) in toluene. The plot of optical density decay and fitting with first-order kinetics of **8a** (b) and **8b** (d) in toluene. Estimated half-life times were shown.

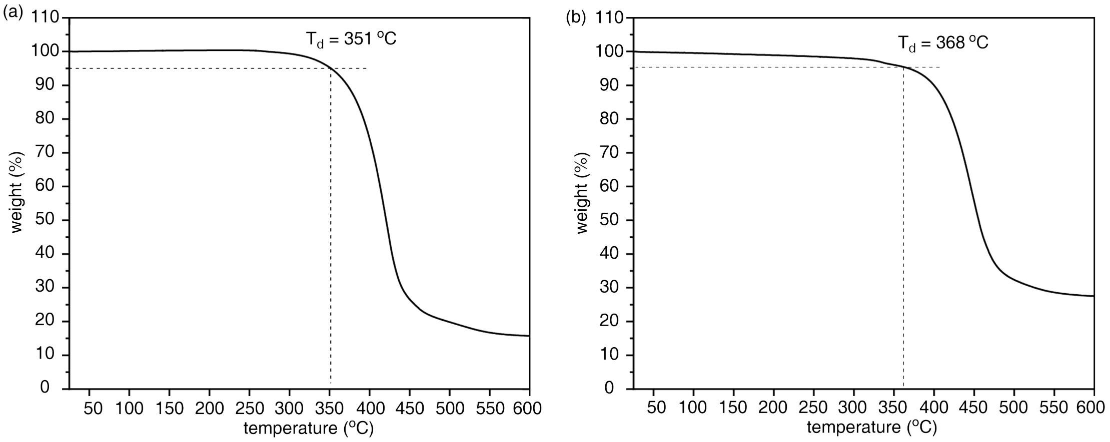

Figure S6. Thermogravimetric analysis curves of (a) **8a** and (b) **8b** at the heating rate of 10 °C /min under N_2 atmosphere.

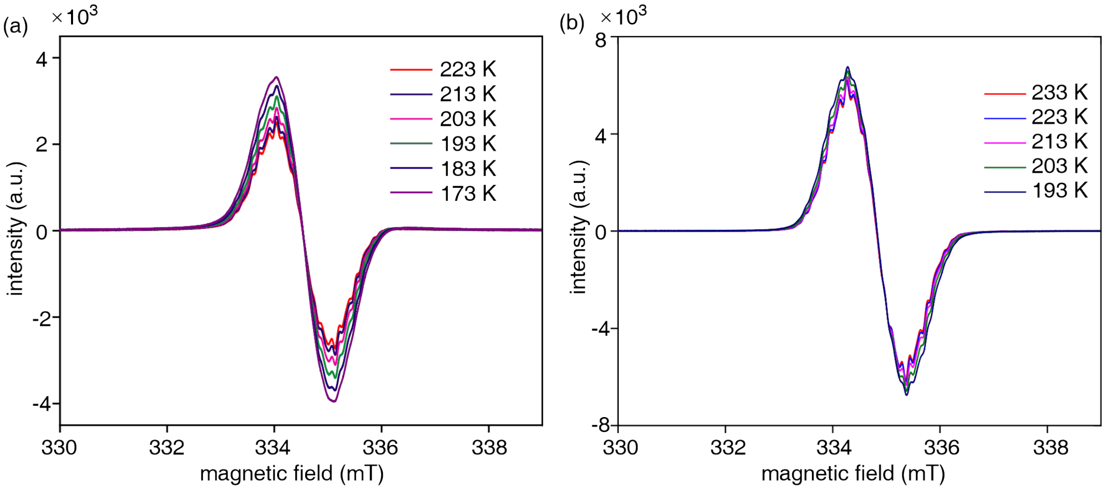

Figure S7. VT-ESR spectra of (a) **8a** at 173-223 K and (b) **8b** at 193-233 K in toluene.

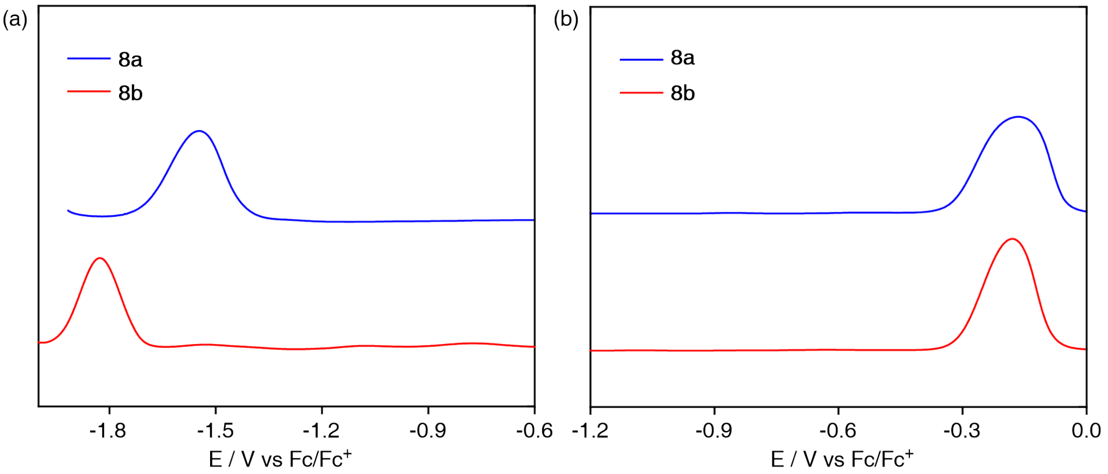

Figure S8. Differential pulse voltammograms of **8a** and **8b** (a) measured in THF and (b) measured in DCM.

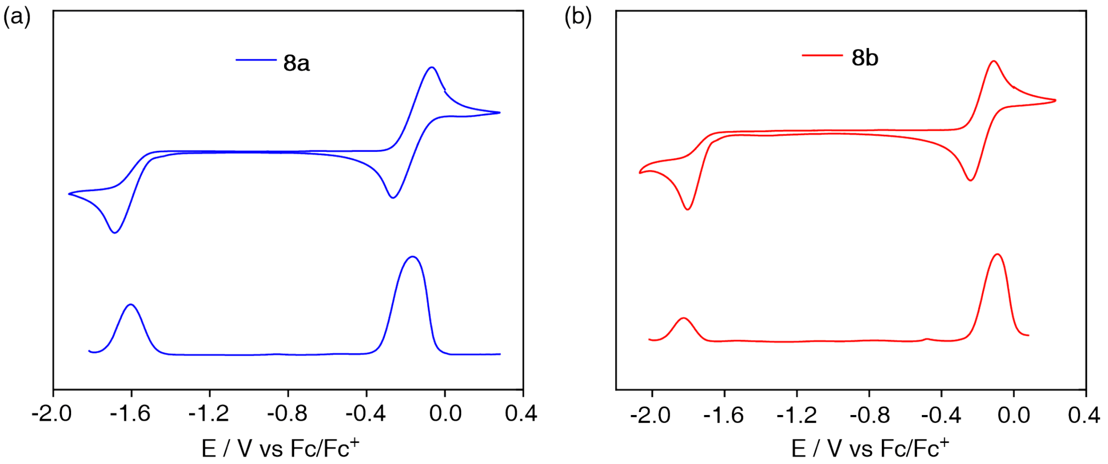

Figure S9. Cyclic voltammograms and differential pulse voltammograms of **8a** (a) and **8b** (b) measured in DCM.

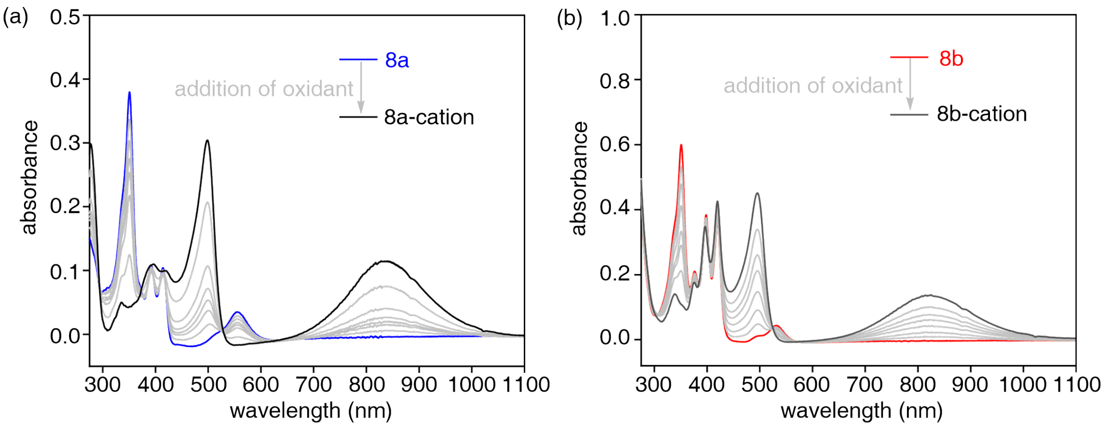

Figure S10. Absorption spectral change upon oxidative titration of (a) **8a** and (b) **8b**.

3. X-ray crystallographic data

The single crystals of **8a** and **8b** suitable for X-ray crystallographic analysis were obtained by diffusion of degassed methanol into the toluene solution of **8a** and isopropanol into the toluene solution of **8b** in glovebox at room temperature. Despite of extensive efforts on the optimization of crystal growth condition, the quality of crystal for **8b** is not satisfied, but represented the best data set that can be collected (Table S4). The single crystal of **7b** suitable for X-ray crystallographic analysis was obtained by slow diffusion of methanol into the chloroform solution of **7b** in air at room temperature. The single crystal X-ray diffraction studies were performed on the XtaLAB Synergy diffractometer equipped with Hypix6000HE detector using Cu Kα radiation (λ = 1.54184 Å). The obtained diffraction data were processed by the program suite CrysAlispro (Rigaku Oxford Diffraction, CrysAlisPro Software system, version 1.171.40_64.53, Rigaku Corporation, Oxford, UK, 2019). The structures were solved with dual-space method using SHELXT program[4] and refined with non-linear least square method using SHELXL program[5] embedded in the program suite OLEX2.[6] For more detailed information about diffraction data collection and refinement parameters, see Table S1 for **7b**, Table S2 for **8a**, Table S5 for **8b**. The crystallographic data were deposited in Cambridge Crystallographic Data Centre (CCDC 2213871 for **7b**, CCDC 2213870 for **8a**, CCDC 2213869 for **8b**). The data can be achieved free of charge from www.ccdc.cam.ac.uk/data_request/cif.

Table S1. Crystal data and structure refinement for **7b** at 100 K.

Data deposition	CCDC 2213871
Empirical formula	$C_{60}H_{64}OSi$
Formula weight	829.20
Temperature/K	100.01(10)
Crystal system	monoclinic
Space group	$P2_1/c$
Unit cell dimensions	$a = 22.2041(5)$ Å
	$b = 17.5850(4)$ Å
	$c = 12.6494(3)$ Å
	$\alpha = 90$ °
	$\beta = 105.508(2)$ °
	$\gamma = 90$ °
Volume/ Å^3	4759.26(19)
Z	4
ρ_{calc}g/cm^3	1.157
μ/mm^{-1}	0.732
F(000)	1784.0
Crystal size/mm^3	0.1 × 0.075 × 0.05
Radiation	Cu Kα (λ = 1.54184)
Independent reflections	9826
Data/restraints/parameters	9826/30/573
Goodness-of-fit on F^2	1.064
R indices (all data)	$R_1 = 0.1267$, $wR_2 = 0.2949$

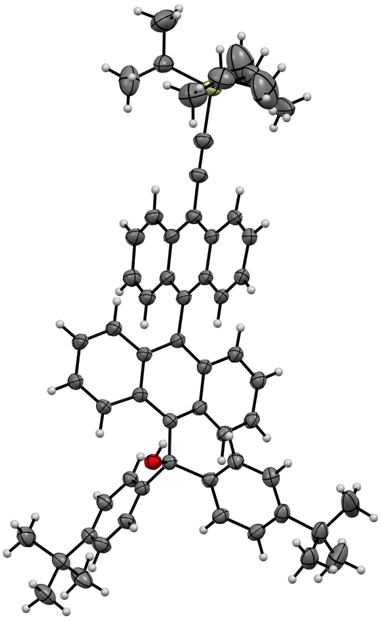

Figure S11. Crystal structure of **7b**.

Table S2. Crystal data and structure refinement for **8a** at 293 K.

Data deposition	CCDC 2213870
Empirical formula	$C_{46}H_{55}Si$
Formula weight	635.99
Temperature/K	293(2)
Crystal system	monoclinic
Space group	$C2/c$
Unit cell dimensions	a = 27.4174(10) Å
	b = 12.3393(4) Å
	c = 24.1653(7) Å
	α = 90 °
	β = 108.966(4) °
	γ = 90 °
Volume/ Å^3	7731.6(5)
Z	8
ρ_{calc}g/cm^3	1.093
μ/mm^{-1}	0.739
F(000)	2760.0
Crystal size/mm^3	0.2 × 0.05 × 0.05
Radiation	Cu Kα (λ = 1.54184)
Independent reflections	7457
Data/restraints/parameters	7457/0/436
Goodness-of-fit on F^2	1.062
R indices (all data)	R_1 = 0.0707, wR_2 = 0.1505

Table S3. The bond lengths of **8a** in single crystal structure.

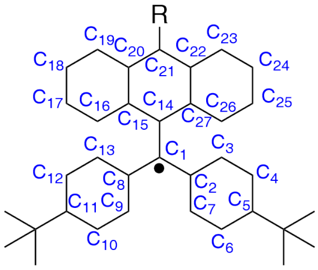

Chemical bond	Bond length (Å)	Chemical bond	Bond length (Å)
C_1-C_2	1.451(3)	C_2-C_3	1.406(3)
C_3-C_4	1.383(3)	C_4-C_5	1.402(3)
C_5-C_6	1.384(3)	C_6-C_7	1.389(3)
C_2-C_7	1.409(3)	C_1-C_8	1.442(3)
C_8-C_9	1.415(2)	C_9-C_{10}	1.373(3)
C_{10}-C_{11}	1.400(3)	C_{11}-C_{12}	1.400(3)
C_{12}-C_{13}	1.370(3)	C_8-C_{13}	1.414(3)
C_1-C_{14}	1.498(2)	C_{14}-C_{15}	1.404(3)
C_{15}-C_{16}	1.429(3)	C_{16}-C_{17}	1.355(3)
C_{17}-C_{18}	1.418(3)	C_{18}-C_{19}	1.361(3)
C_{19}-C_{20}	1.424(3)	C_{15}-C_{20}	1.435(2)
C_{20}-C_{21}	1.411(3)	C_{21}-C_{22}	1.409(3)
C_{22}-C_{23}	1.427(3)	C_{23}-C_{24}	1.352(3)
C_{24}-C_{25}	1.420(3)	C_{25}-C_{26}	1.355(3)
C_{26}-C_{27}	1.426(3)	C_{22}-C_{27}	1.439(3)
C_{14}-C_{27}	1.408(3)		

Table S4. The selected cultivation condition of single crystal **8b**.

Entry	Method	Solvent	Concentration (mg/mL)	Temperature	Result
1	solvent diffusion	toluene/ MeOH	10	rt	powder
2	solvent diffusion	toluene/ MeOH	10	-20 ºC	powder
3	solvent diffusion	toluene/ *i*PrOH	10	rt	thin plate crystal
4	solvent diffusion	toluene/ *i*PrOH	10	-20 ºC	thin plate crystal
5	solvent diffusion	toluene/ CH_3CN	10	rt	powder
6	solvent diffusion	toluene/ CH_3CN	10	-20 ºC	powder
7	solvent diffusion	toluene/ hexane	10	rt	solution
8	solvent diffusion	toluene/ hexane	10	-20 ºC	solution
9	solvent diffusion	toluene/ *i*PrOH	5	rt	thin plate crystal
10	solvent diffusion	toluene/ *i*PrOH	20	rt	thin plate crystal
11	slow cooling	toluene/ *i*PrOH (2:1)	5 (stock solution)	-4 ºC	solution
12	slow cooling	toluene/ *i*PrOH (1:1)	5 (stock solution)	-4 ºC	solution
13	slow cooling	toluene/ *i*PrOH (2:3)	5 (stock solution)	-4 ºC	solution
14	slow cooling	toluene/ *i*PrOH (1:2)	5 (stock solution)	-4 ºC	solution
15	slow cooling	toluene/ *i*PrOH (1:3)	5 (stock solution)	-4 ºC	thin plate crystal

Table S5. Crystal data and structure refinement for **8b** at 160 K.

Data deposition	CCDC 2213869
Empirical formula	$C_{60}H_{63}Si$
Formula weight	812.19
Temperature/K	160.15
Crystal system	monoclinic
Space group	$P2_1/c$
Unit cell dimensions	a = 22.5678(8) Å
	b = 17.3752(8) Å
	c = 12.8103(6) Å
	α = 90 °
	β = 106.295(5) °
	γ = 90 °
Volume/ $Å^3$	4821.4(4)
Z	4
$\rho_{calc}g/cm^3$	1.119
μ/mm^{-1}	0.697
$F(000)$	1748.0
Crystal size/mm^3	0.1 × 0.03 × 0.03
Radiation	Cu Kα (λ = 1.54184)
Independent reflections	7116
Data/restraints/parameters	7116/182/633
Goodness-of-fit on F^2	1.004
R indices (all data)	R_1 = 0.1410, wR_2 = 0.2381

Table S6. The bond lengths of **8b** in single crystal structure.

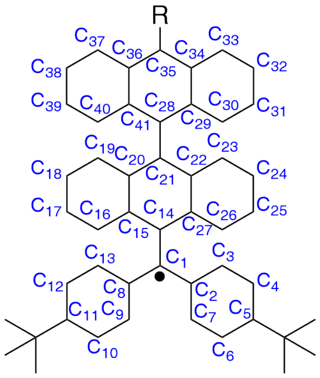

Chemical bond	Bond length (Å)	Chemical bond	Bond length (Å)
C_1-C_2	1.457(6)	C_2-C_3	1.380(7)
C_3-C_4	1.378(7)	C_4-C_5	1.390(5)
C_5-C_6	1.395(7)	C_6-C_7	1.371(7)
C_2-C_7	1.408(5)	C_1-C_8	1.452(6)
C_8-C_9	1.389(5)	C_9-C_{10}	1.368(7)
C_{10}-C_{11}	1.401(8)	C_{11}-C_{12}	1.390(7)
C_{12}-C_{13}	1.371(7)	C_8-C_{13}	1.409(7)
C_1-C_{14}	1.487(5)	C_{14}-C_{15}	1.420(5)
C_{15}-C_{16}	1.422(7)	C_{16}-C_{17}	1.353(6)
C_{17}-C_{18}	1.411(6)	C_{18}-C_{19}	1.337(8)
C_{19}-C_{20}	1.435(6)	C_{15}-C_{20}	1.430(5)
C_{20}-C_{21}	1.399(5)	C_{21}-C_{22}	1.412(5)
C_{22}-C_{23}	1.419(5)	C_{23}-C_{24}	1.350(6)
C_{24}-C_{25}	1.430(6)	C_{25}-C_{26}	1.344(7)
C_{26}-C_{27}	1.429(6)	C_{22}-C_{27}	1.439(5)
C_{14}-C_{27}	1.408(5)	C_{21}-C_{28}	1.508(5)
C_{28}-C_{29}	1.391(7)	C_{29}-C_{30}	1.409(7)
C_{30}-C_{31}	1.362(7)	C_{31}-C_{32}	1.419(6)
C_{32}-C_{33}	1.358(8)	C_{33}-C_{34}	1.418(7)
C_{29}-C_{34}	1.455(6)	C_{34}-C_{35}	1.398(7)
C_{35}-C_{36}	1.398(7)	C_{36}-C_{37}	1.432(7)
C_{37}-C_{38}	1.347(7)	C_{38}-C_{39}	1.423(6)
C_{39}-C_{40}	1.352(7)	C_{28}-C_{41}	1.399(7)
C_{36}-C_{41}	1.452(5)	C_{40}-C_{41}	1.414(7)

4. Theoretical calculations

The density functional theory (DFT) calculations were performed with the Gaussian 09 program suite (Revision A.1).[7] All calculations were performed using DFT method with unrestricted Becke's three-parameter hybrid exchange functionals and the Lee-Yang-Parr correlation functional (UB3LYP) or UM062X[8] functional employing 6-31G(d), 6-31G(d,p) or EPR-III basis set for all atoms.[9-14] The geometry optimizations were performed at UB3LYP/6-31G(d,p) level of theory. The HFCCs of **8a** and **8b** in toluene were calculated by UM062X/EPR-III theory level. Time-dependent DFT (TD-DFT) for **8a** and **8b** were carried out at UB3LYP/6-31G(d,p) theory level.

4.1 Molecular orbital profiles and spin density distribution

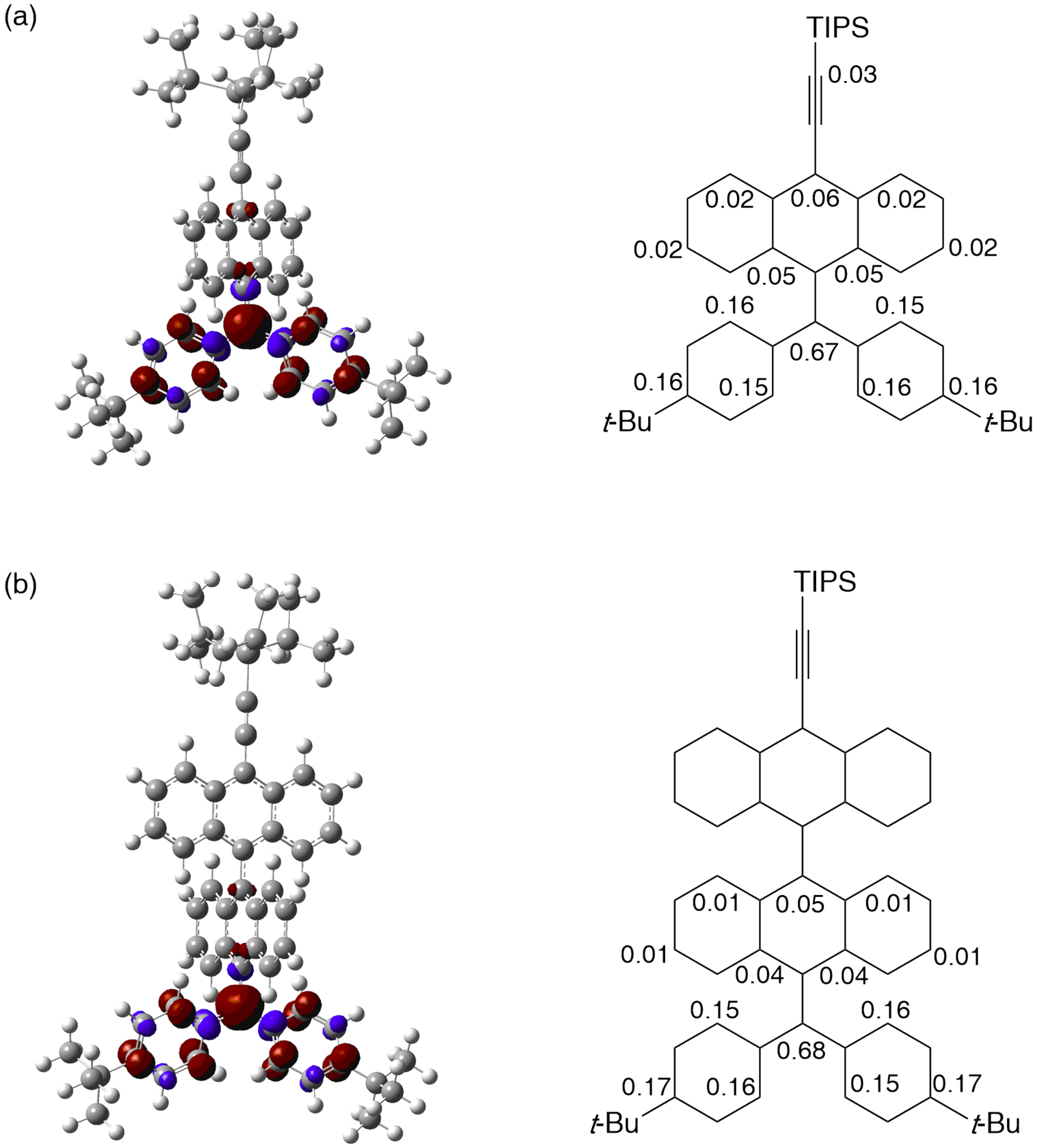

Figure S12. Calculated spin density distribution and Mülliken spin density (msd) values for (a) **8a** and (b) **8b** at UB3LYP/6-31G(d,p) level of theory.

4.2 TD-DFT calculations

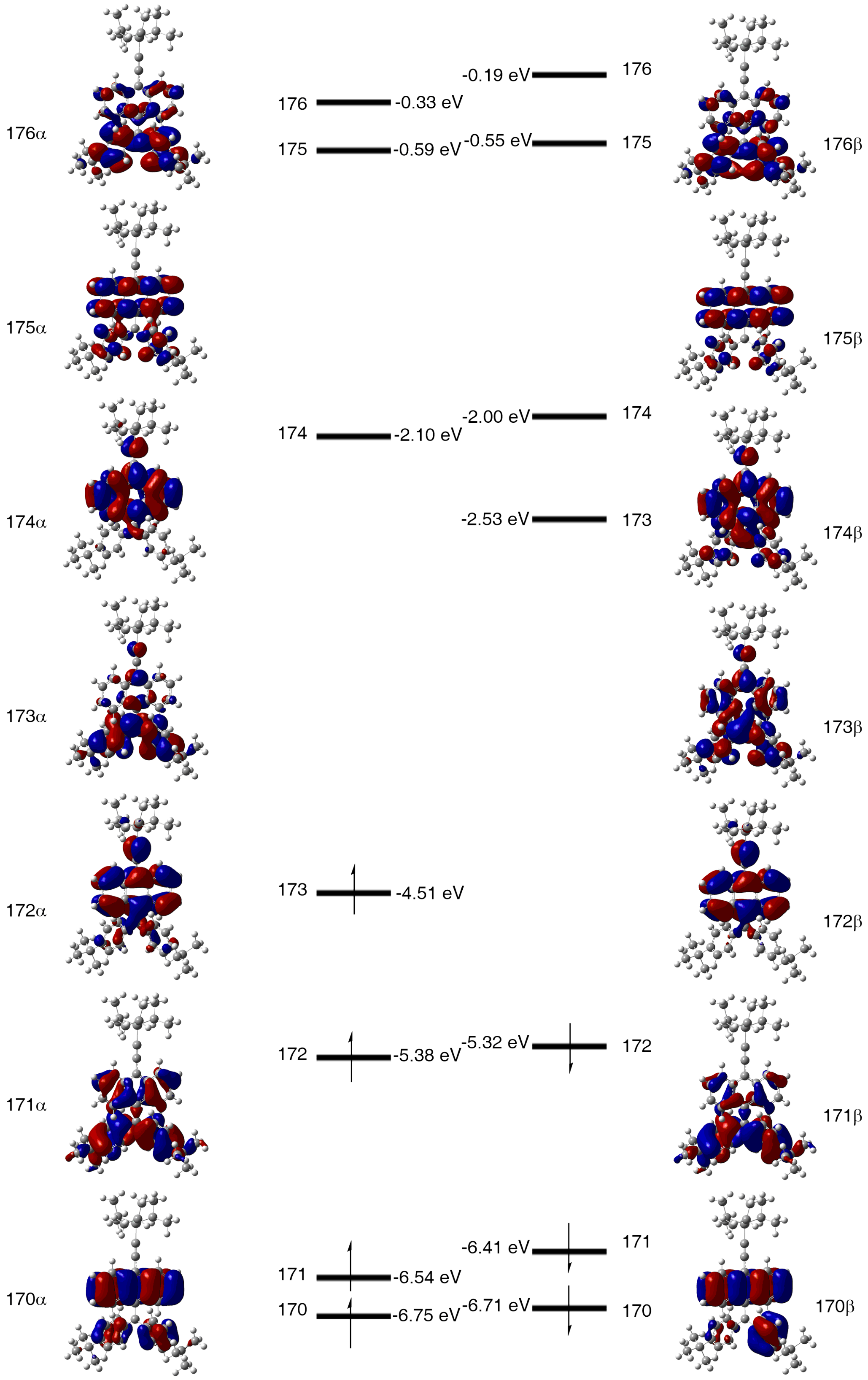

Figure S13. Molecular orbital diagram of **8a** from TD-DFT calculation at UB3LYP/6-31G(d,p) level of theory.

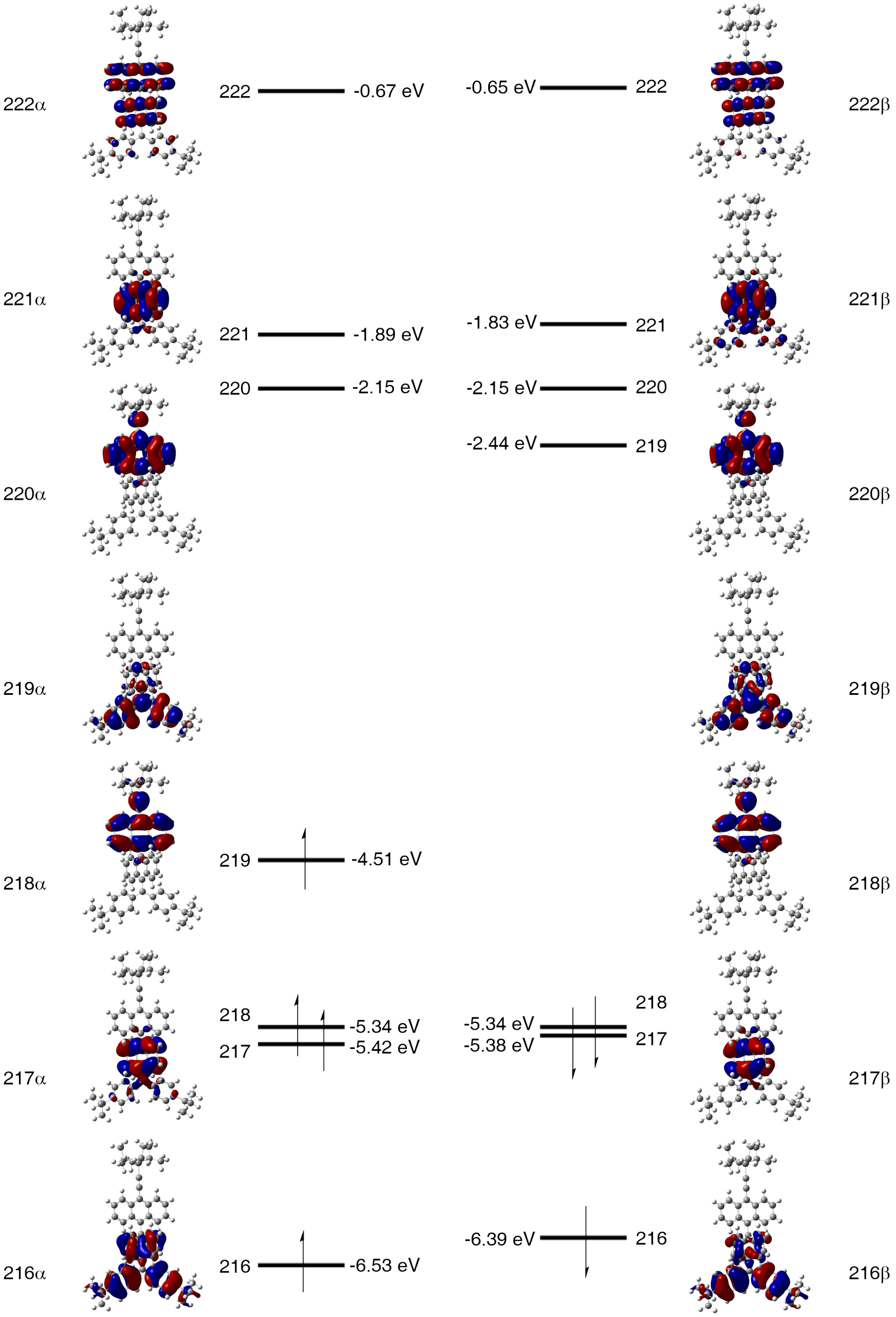

Figure S14. Molecular orbital diagram of **8b** from TD-DFT calculation at UB3LYP/6-31G(d,p) level of theory.

Table S7. Calculated electronic transitions for **8a**.

No	Wavelength (nm)	Oscillator strength	Major contributions
1	856.13	0.0048	172α-174α (20%), 173α-174α (41%), 172β-173β (23%), 172β-174β (16%)
2	664.73	0.0880	172α-174α (20%), 173α-174α (58%), 172β-173β (14%)
3	550.93	0.0655	172α-174α (12%), 172β-173β (60%), 172β-174β (27%)
4	427.15	0.2691	172α-174α (47%), 172β-174β (49%)
5	338.23	0.0516	173α-178α (53%), 173α-179α (7%), 169β-173β (24%), 172β-175β (3%)

Table S8. Calculated electronic transitions for **8b**.

No	Wavelength (nm)	Oscillator strength	Major contributions
1	760.55	0.0029	217α-221α (24%), 219α-221α (35%), 217β-219β (16%), 217β-221β (23%)
2	610.24	0.0607	217α-221α (16%), 219α-221α (64%), 217β-219β (11%), 217β-221β (9%)
3	534.64	0.0392	217α-221α (9%), 217β-219β (72%), 217β-221β (17%)
4	437.10	0.4955	218α-220α (47%), 218β-220β (47%)
5	394.30	0.0874	217α-221α (46%), 217β-221β (45%)

4.3 Calculated ESR spectra

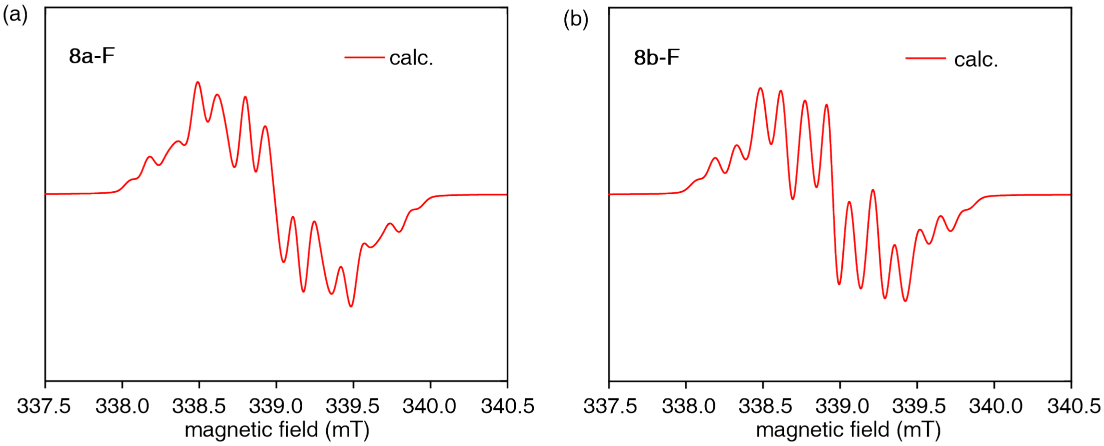

Figure S15. Calculated ESR spectra for (a) **8a-F** and (b) **8b-F** (9.5 GHz).

5. ^{1}H/^{13}C NMR and MS spectra for new compounds

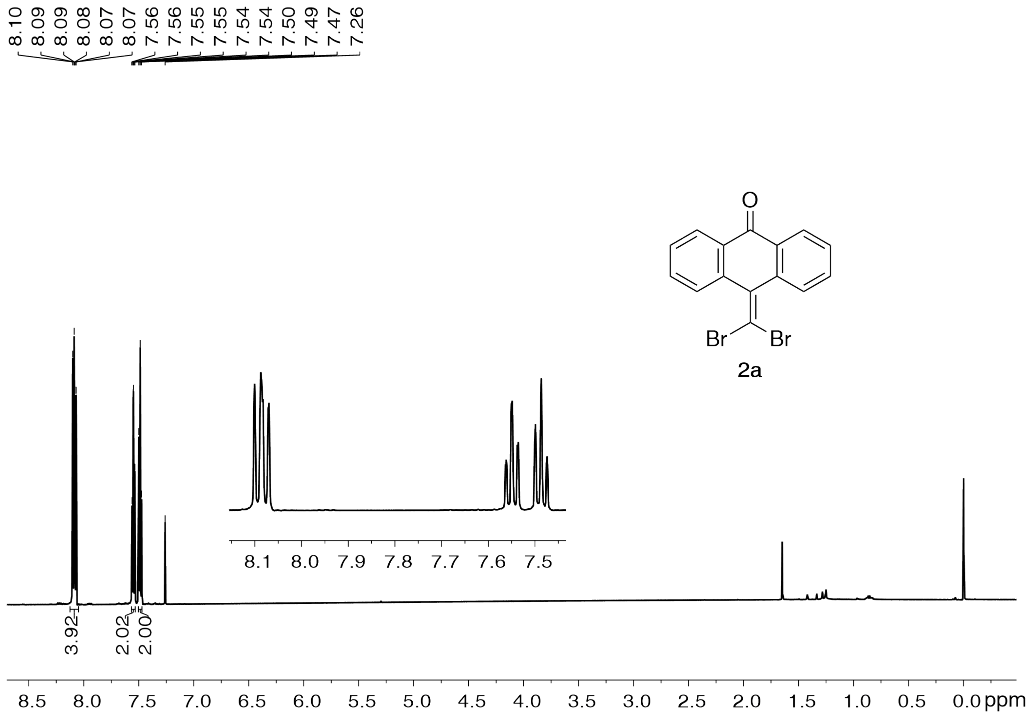

Figure S16. ^{1}H NMR spectrum of **2a** in $CDCl_3$ (600 MHz).

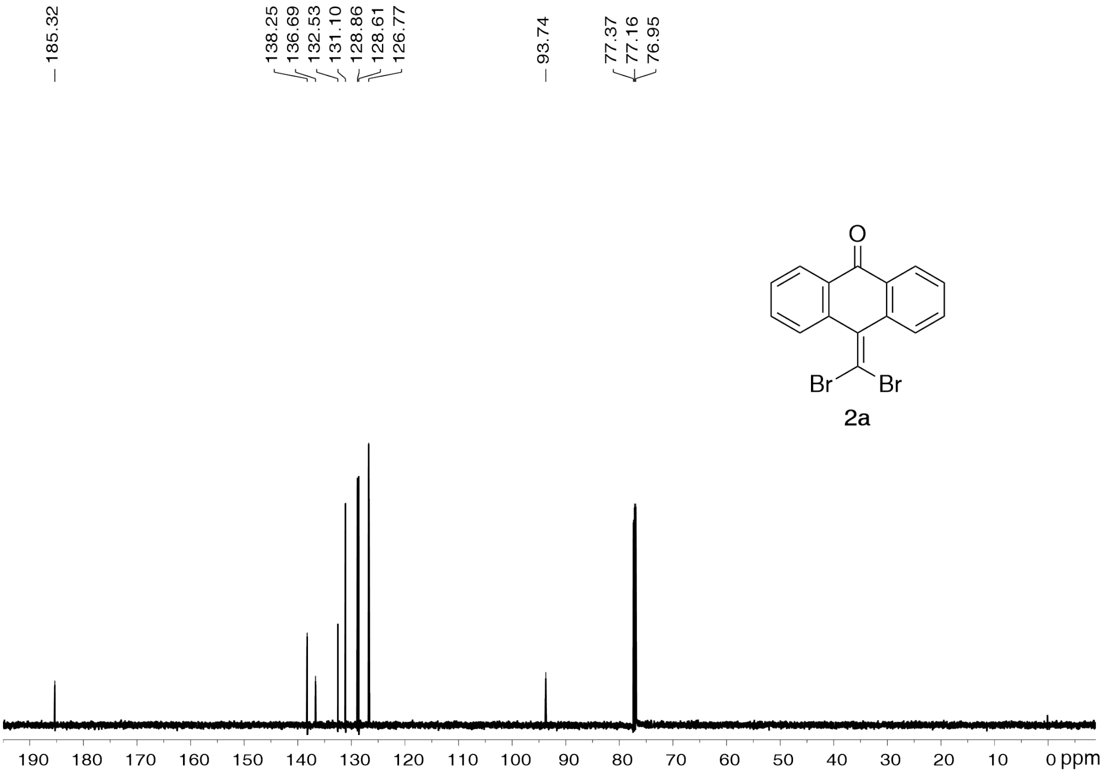

Figure S17. ^{13}C NMR spectrum of **2a** in $CDCl_3$ (150 MHz).

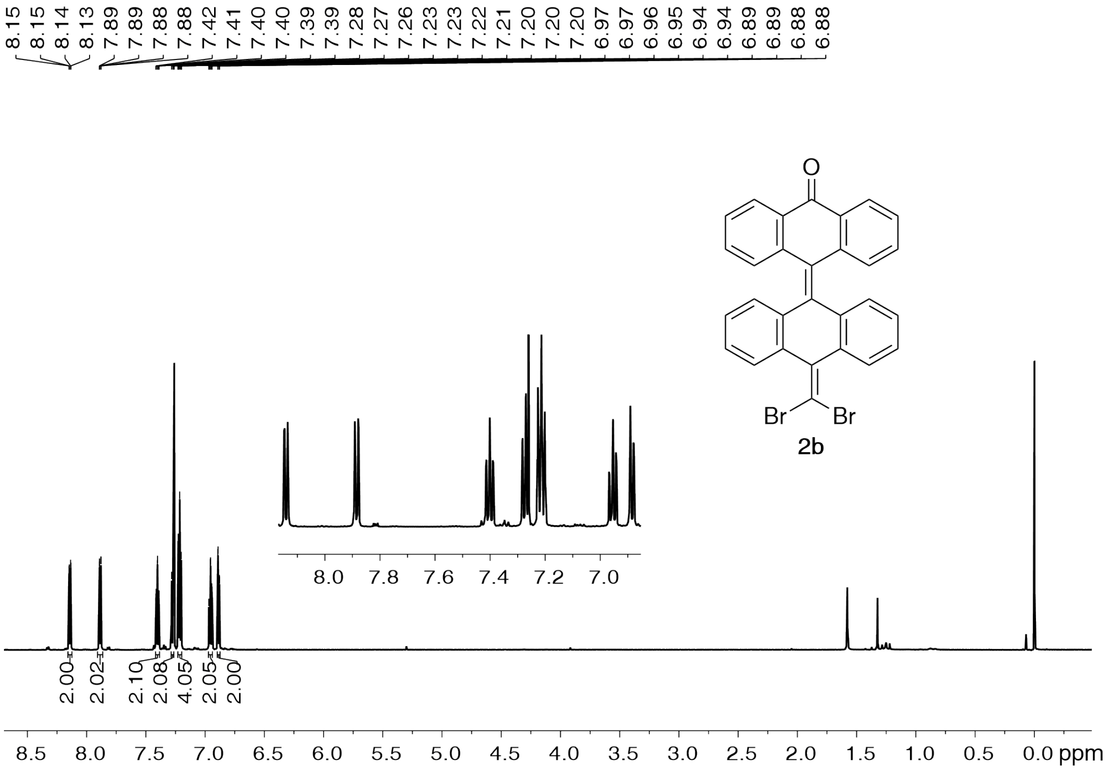

Figure S18. ^{1}H NMR spectrum of **2b** in $CDCl_3$ (600 MHz).

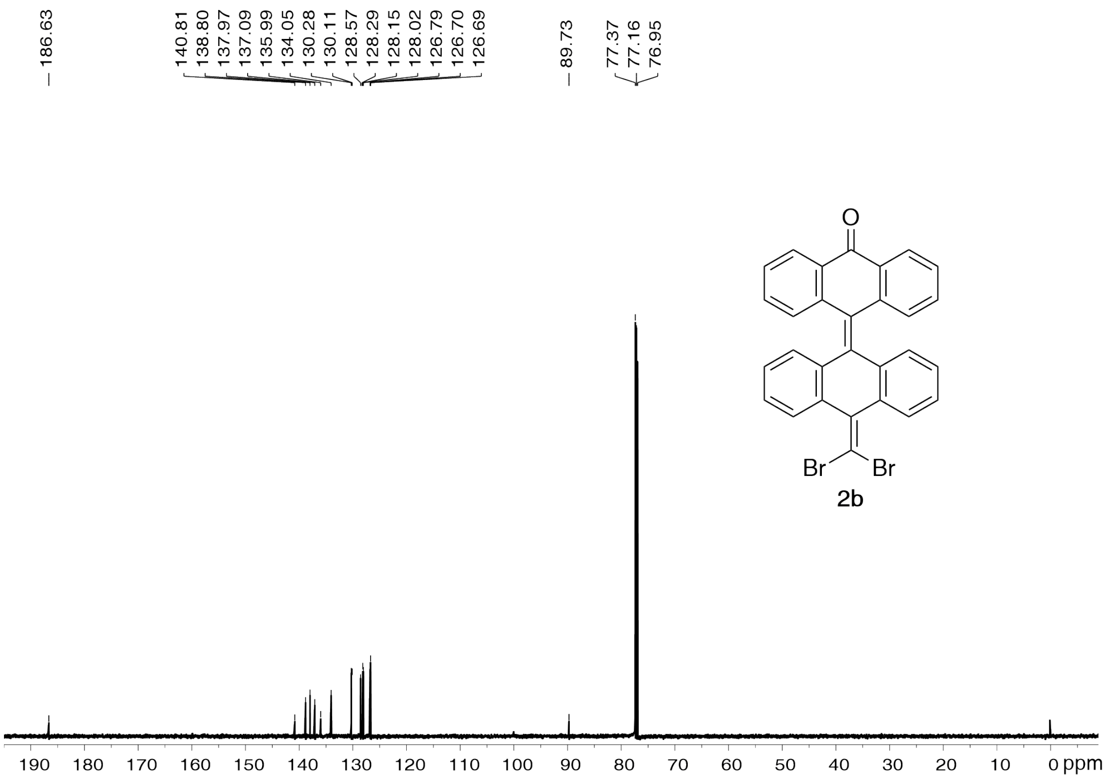

Figure S19. ^{13}C NMR spectrum of **2b** in $CDCl_3$ (150 MHz).

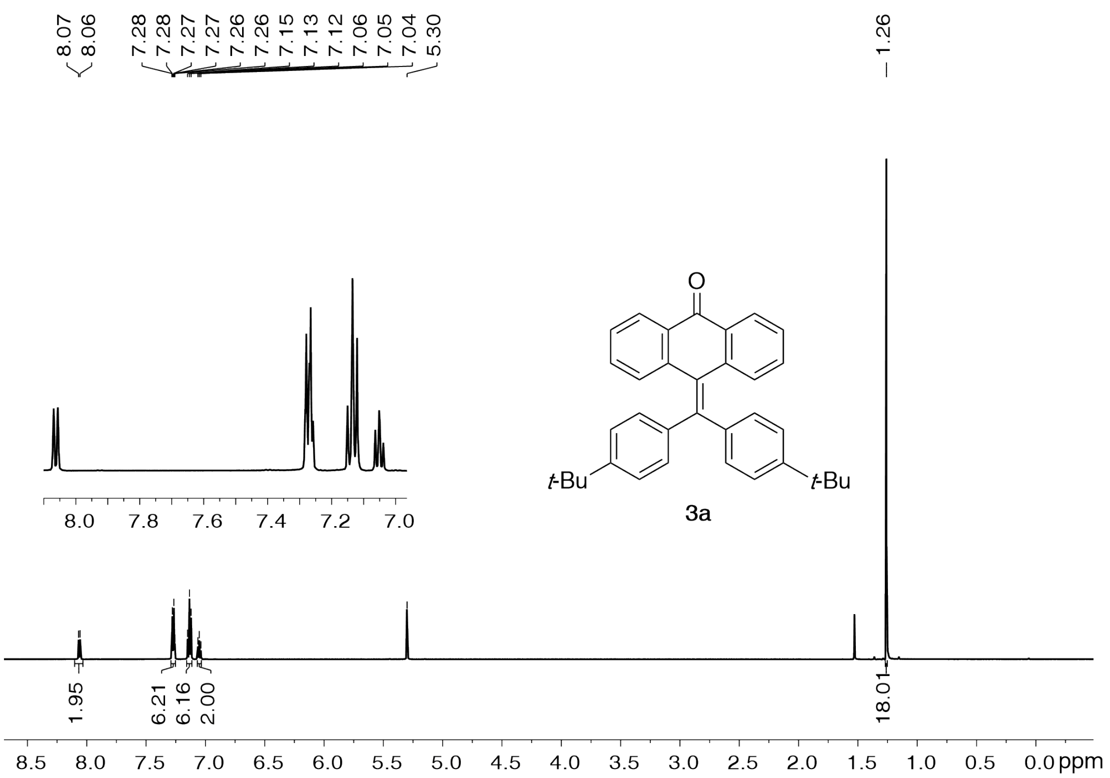

Figure S20. ^{1}H NMR spectrum of **3a** in CD_2Cl_2 (600 MHz).

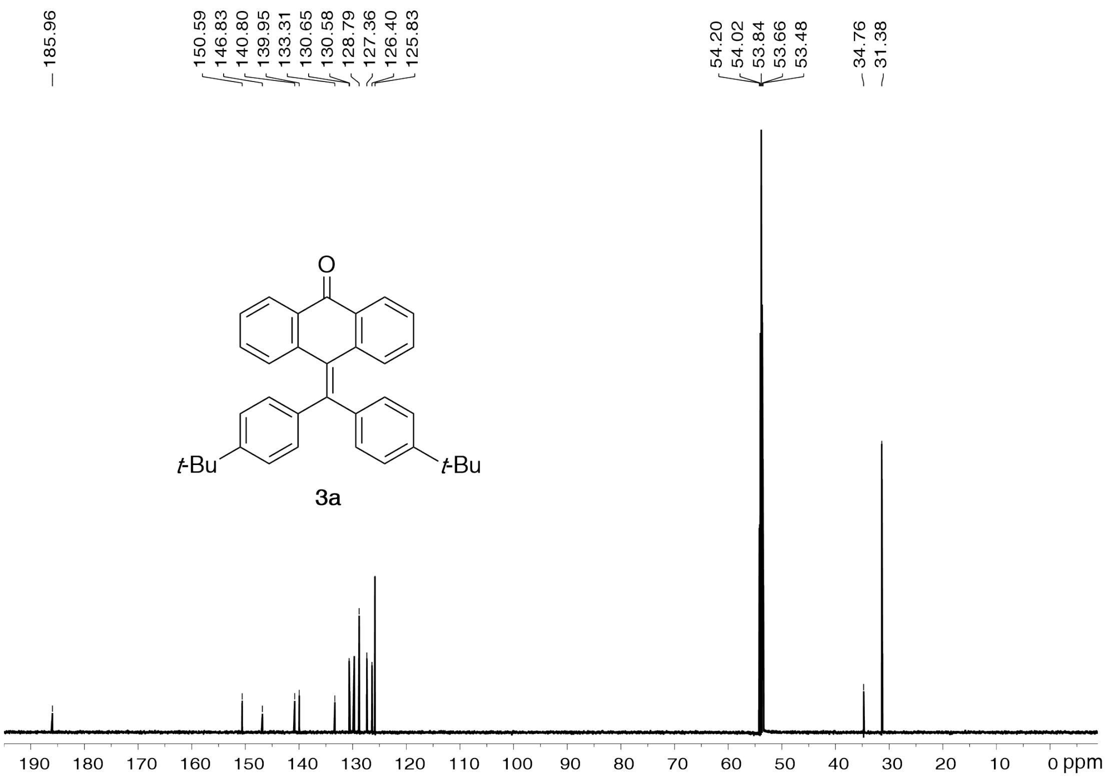

Figure S21. ^{13}C NMR spectrum of **3a** in CD_2Cl_2 (150 MHz).

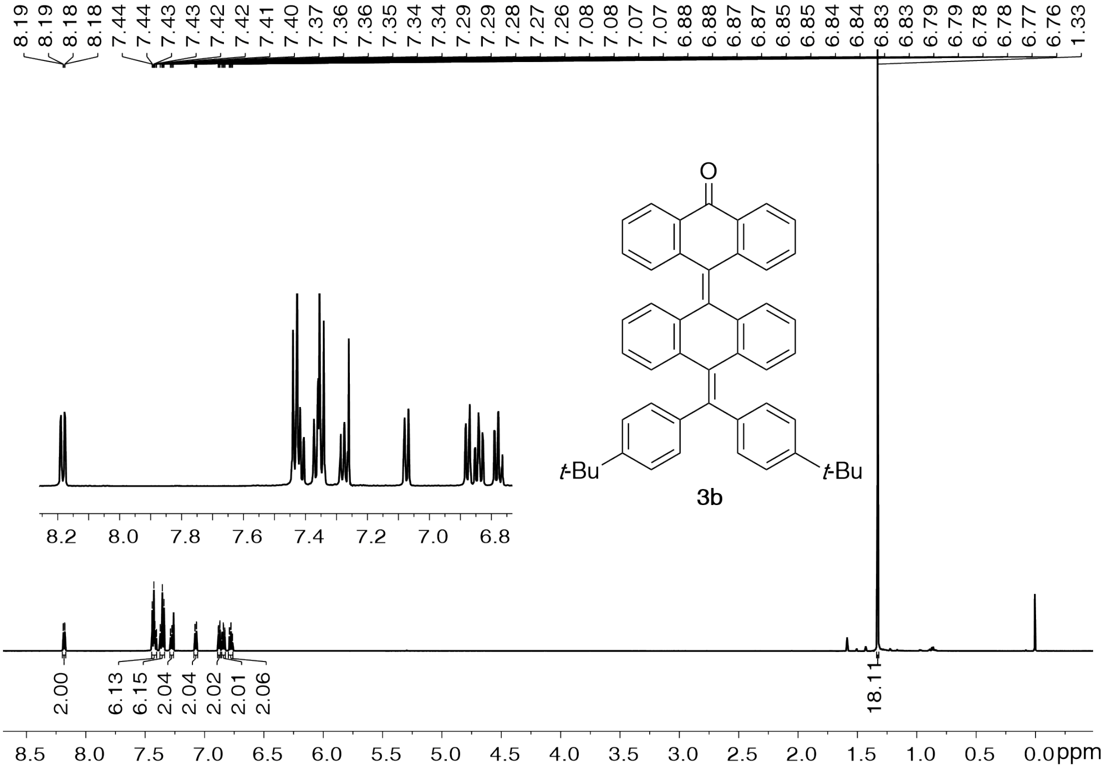

Figure S22. ^{1}H NMR spectrum of **3b** in $CDCl_3$ (600 MHz).

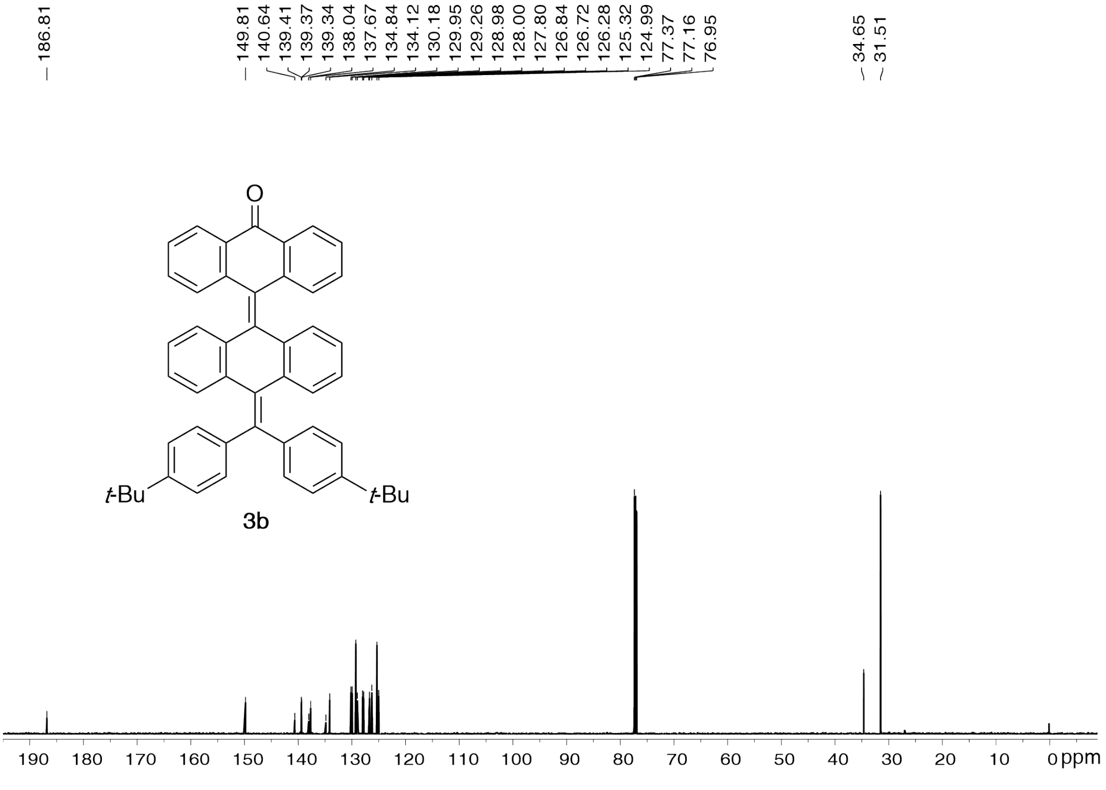

Figure S23. ^{13}C NMR spectrum of **3b** in $CDCl_3$ (150 MHz).

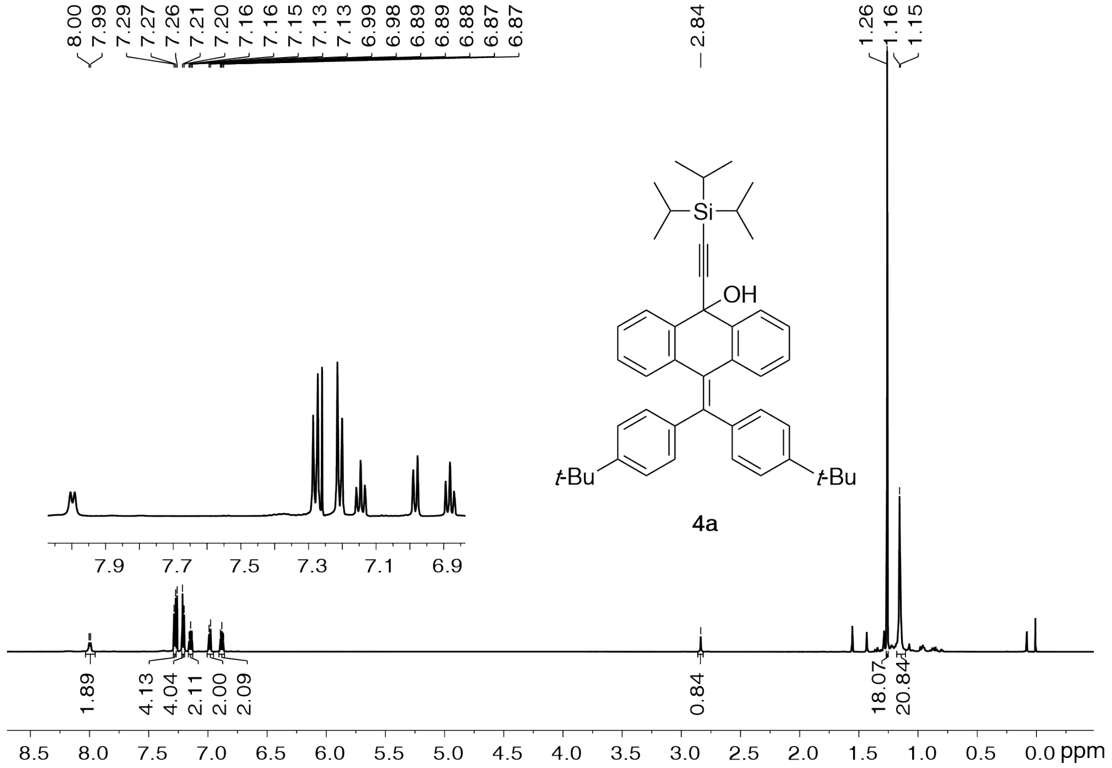

Figure S24. ^{1}H NMR spectrum of **4a** in $CDCl_3$ (600 MHz).

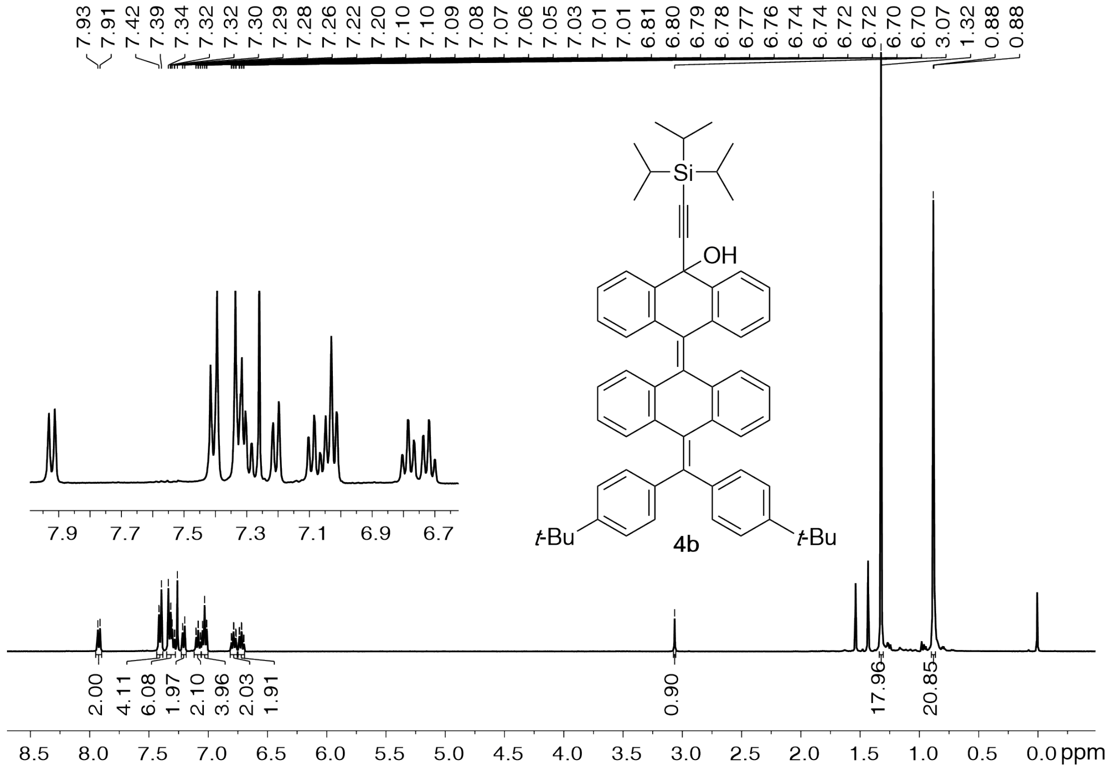

Figure S25. ^{1}H NMR spectrum of **4b** in $CDCl_3$ (600 MHz).

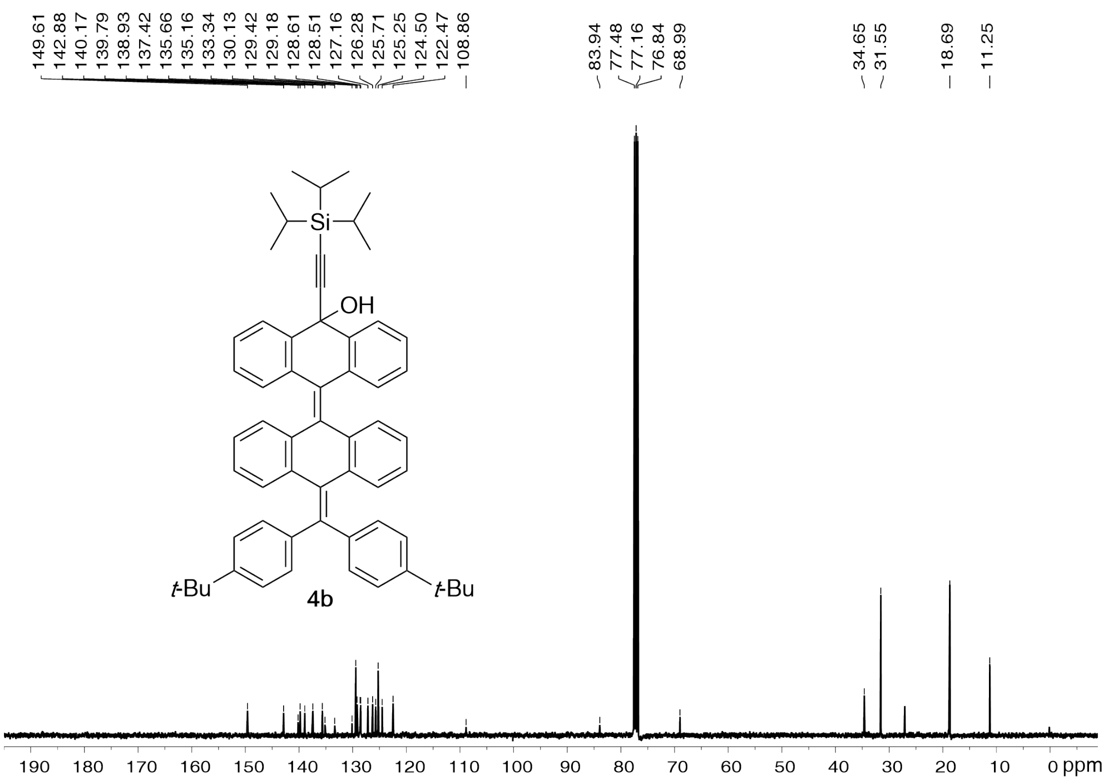

Figure S26. ^{13}C NMR spectrum of **4b** in CDCl$_3$ (150 MHz).

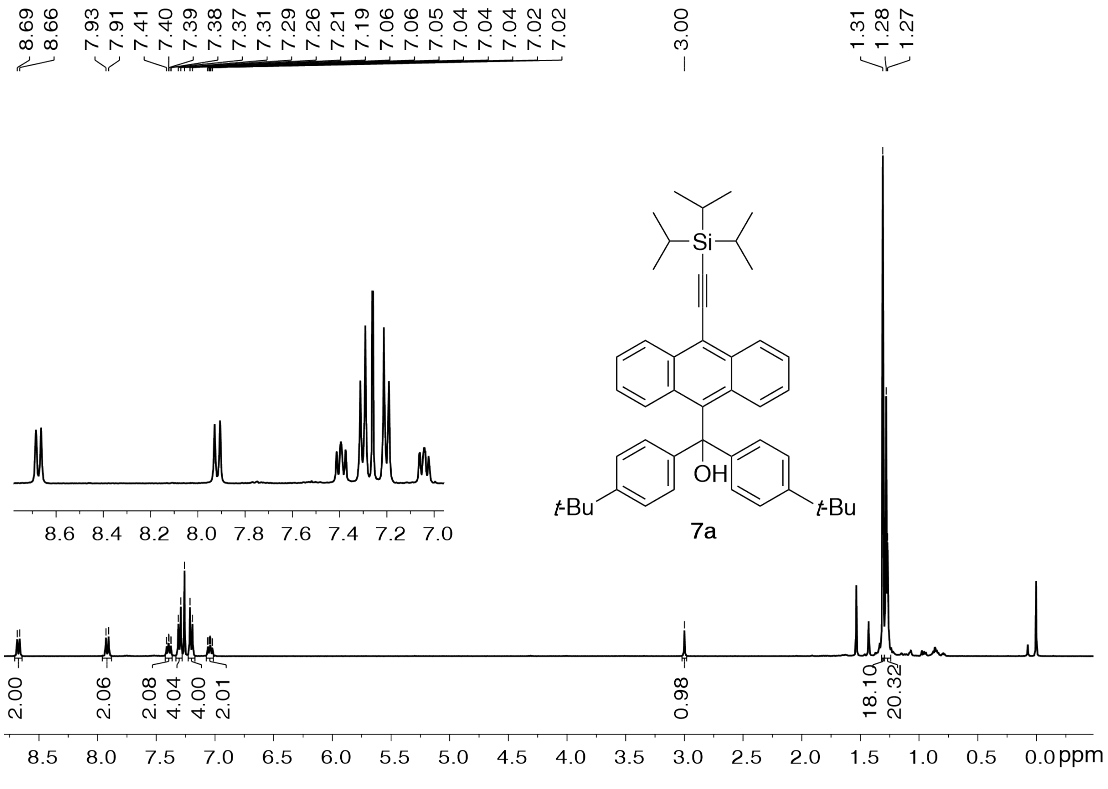

Figure S27. ^{1}H NMR spectrum of **7a** in CDCl$_3$ (400 MHz).

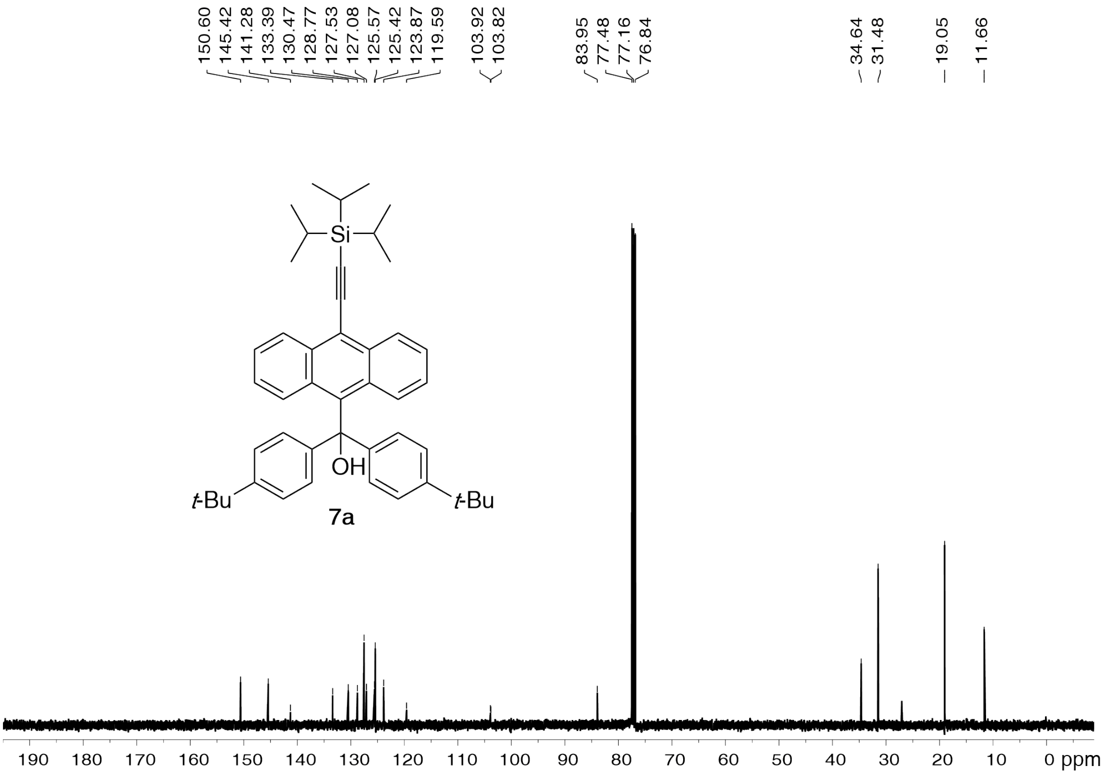

Figure S28. ^{13}C NMR spectrum of **7a** in CDCl$_3$ (100 MHz).

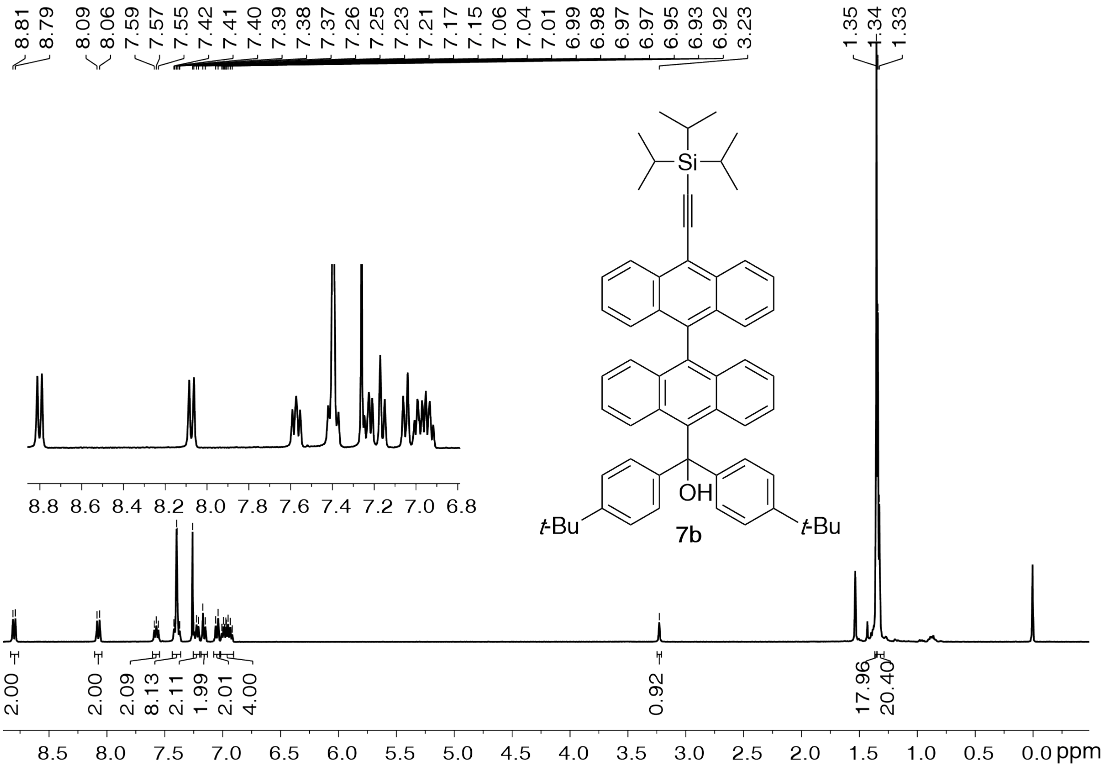

Figure S29. ^{1}H NMR spectrum of **7b** in CDCl$_3$ (400 MHz).

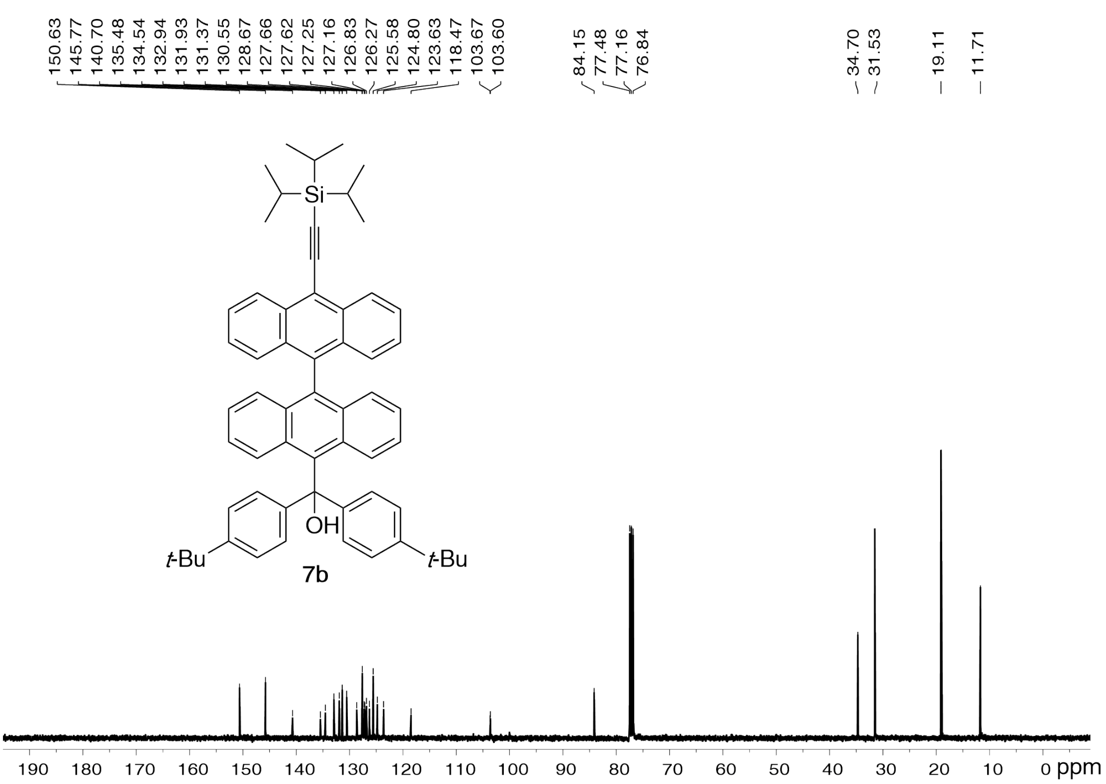

Figure S30. ^{13}C NMR spectrum of **7b** in $CDCl_3$ (100 MHz).

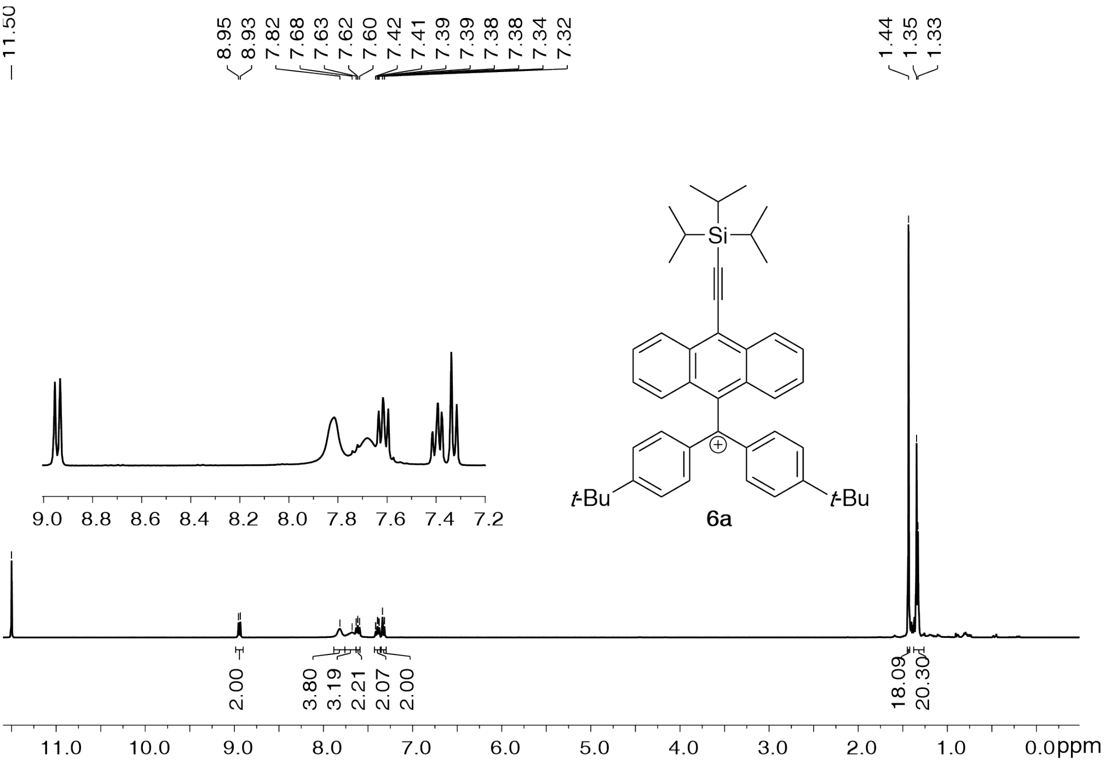

Figure S31. ^{1}H NMR spectrum of **6a** in TFA-d_1 (400 MHz).

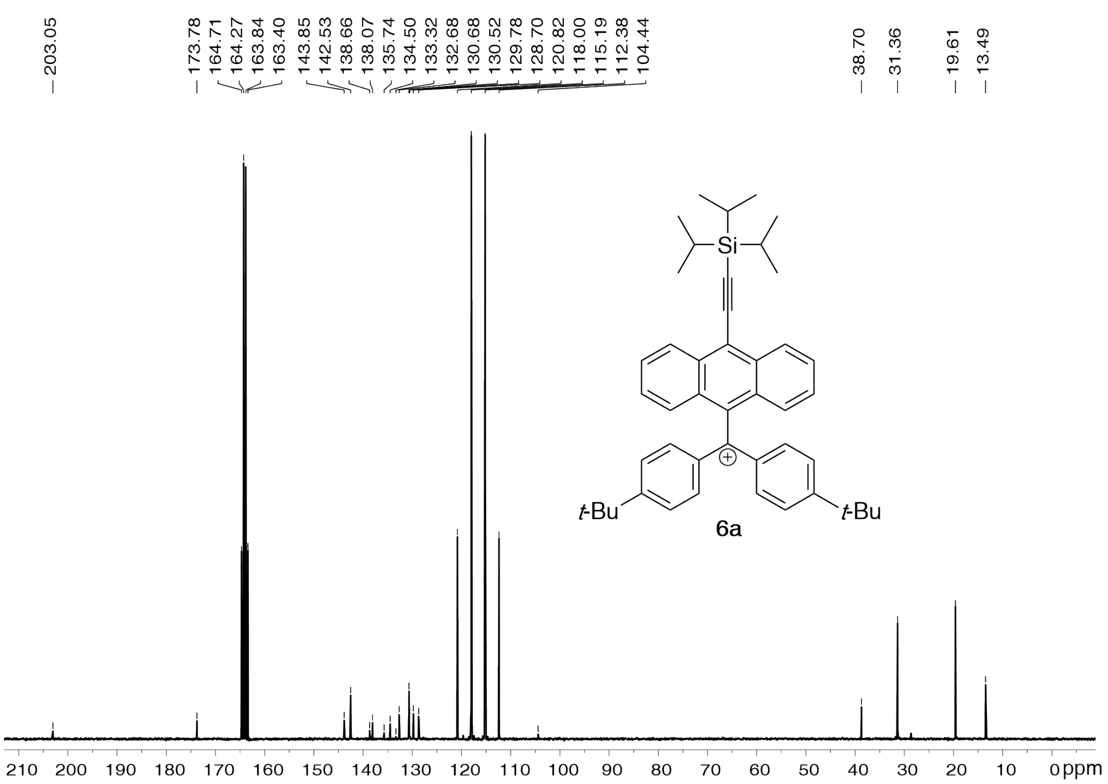

Figure S32. ^{13}C NMR spectrum of **6a** in TFA-d_1 (100 MHz).

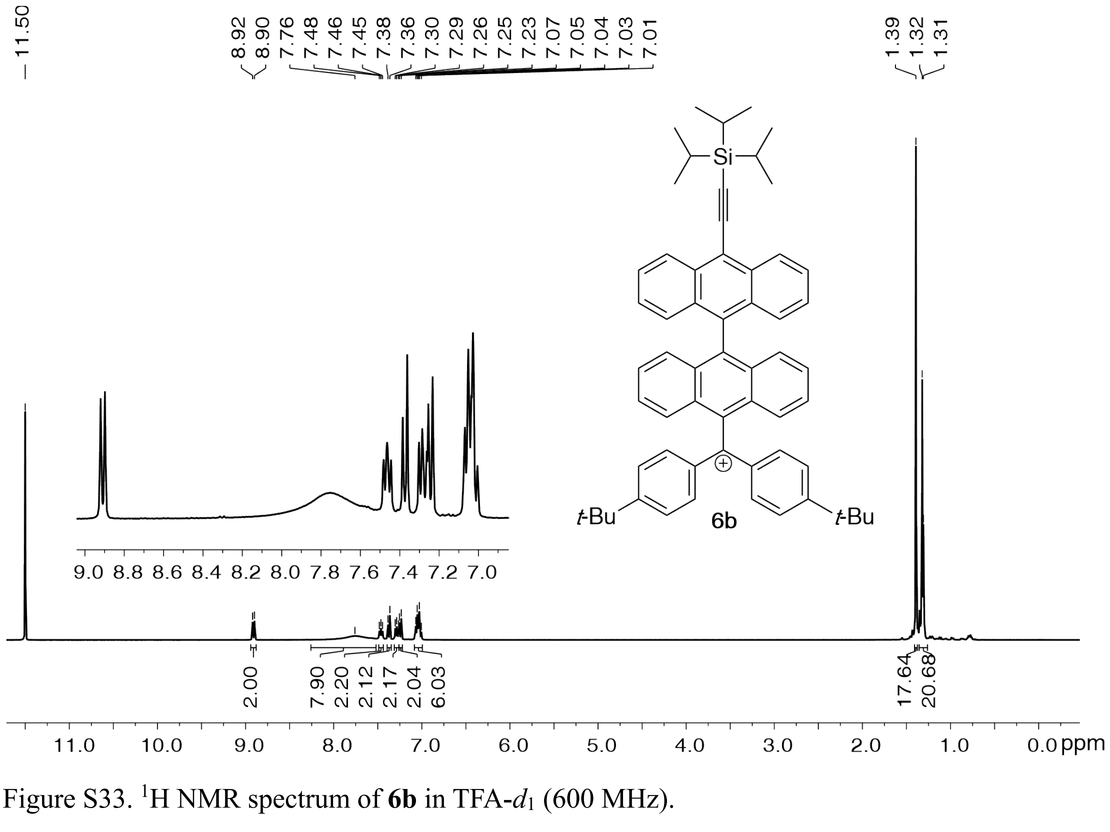

Figure S33. ^{1}H NMR spectrum of **6b** in TFA-d_1 (600 MHz).

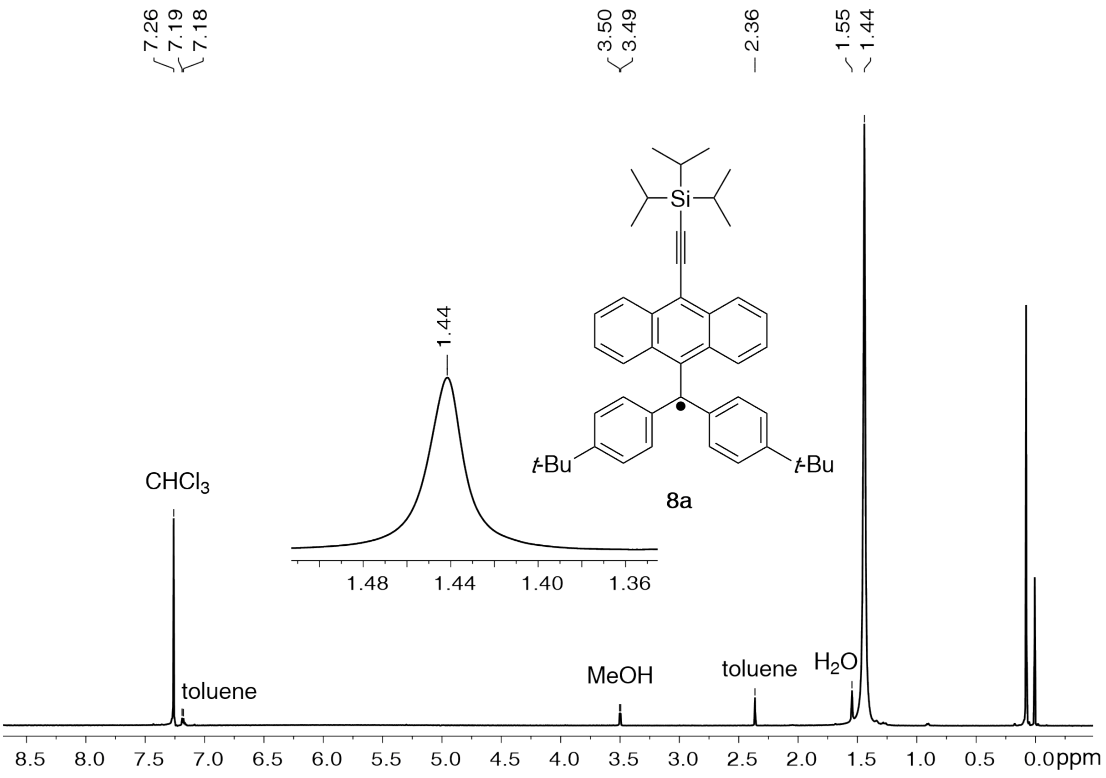

Figure S34. ^{1}H NMR spectrum of **8a** in $CDCl_3$ (600 MHz).

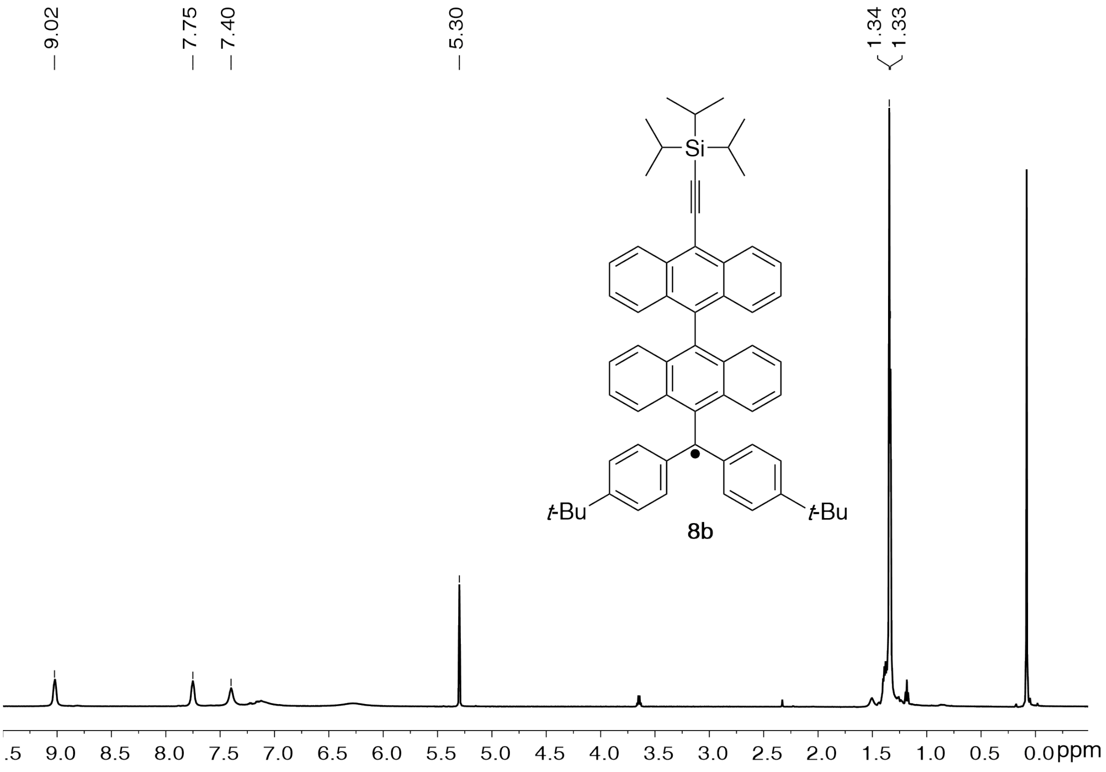

Figure S35. ^{1}H NMR spectrum of **8b** in CD_2Cl_2 (600 MHz).

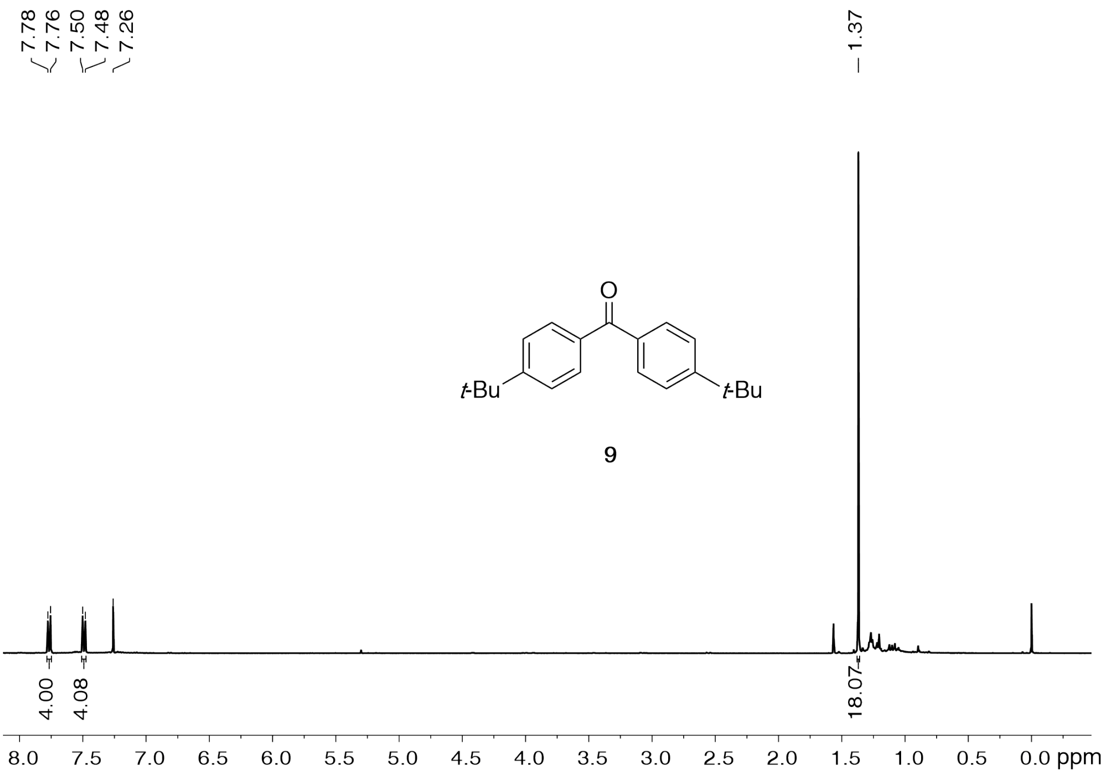

Figure S36. ^{1}H NMR spectrum of **9** in $CDCl_3$ (400 MHz).

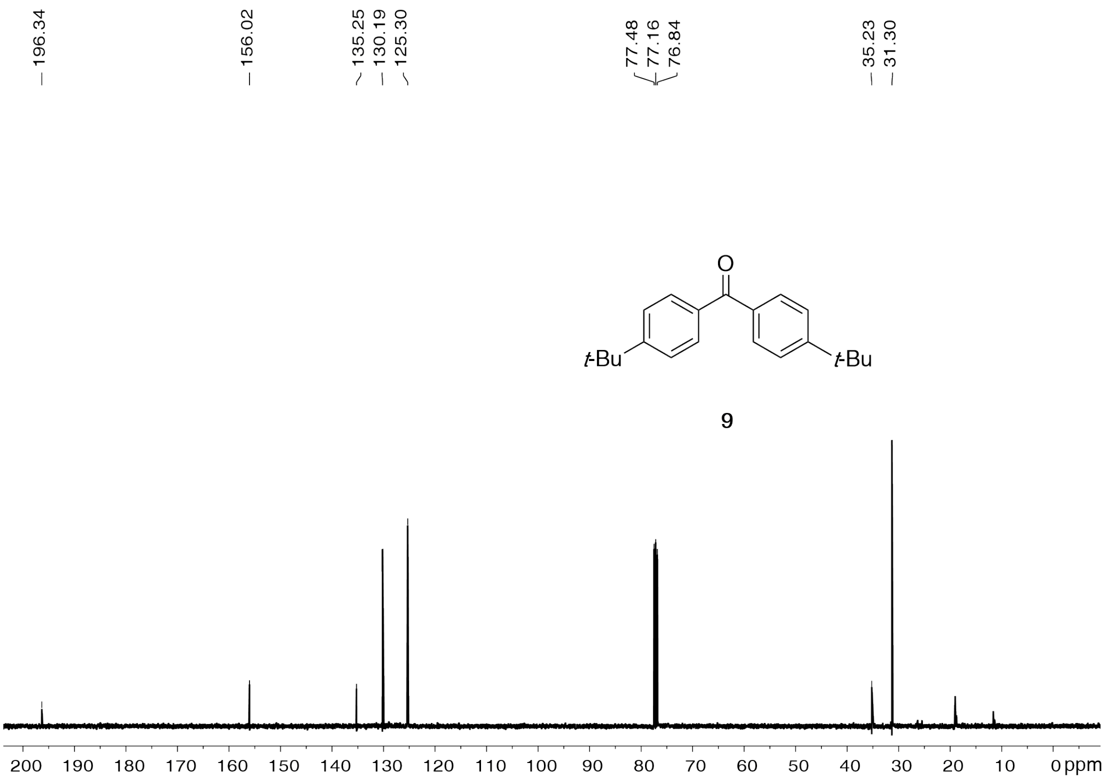

Figure S37. ^{13}C NMR spectrum of **9** in $CDCl_3$ (100 MHz).

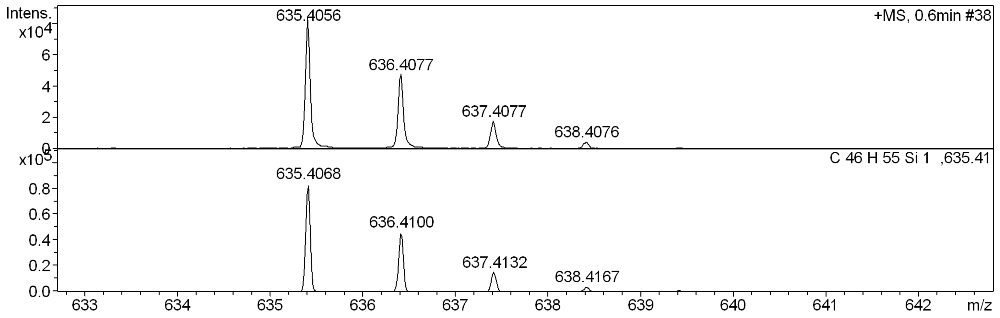

Meas. m/z	#	Formula	Score	m/z	err [mDa]	err [ppm]	mSigma	rdb	e¯ Conf	N-Rule
635.4056	1	C 46 H 55 Si	100.00	635.4068	1.2	1.9	13.8	20.5	even	ok

Figure S38. HR-ESI MS spectrum of compound **8a**.

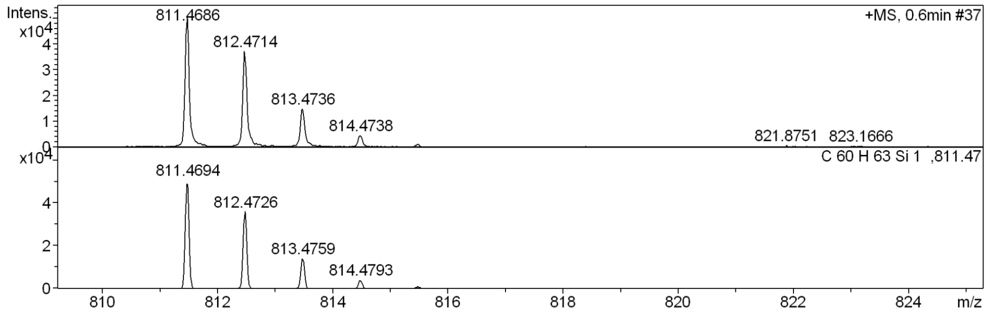

Meas. m/z	#	Formula	Score	m/z	err [mDa]	err [ppm]	mSigma	rdb	e¯ Conf	N-Rule
811.4686	1	C 60 H 63 Si	100.00	811.4694	0.8	1.0	16.9	30.5	even	ok

Figure S39. HR-ESI MS spectrum of compound **8b**.

6. References

1. S. Stoll and A. Schweiger, *J. Magn. Reson.*, 2006, **178**, 42−55.
2. T. Nishiuchi, S. Aibara and T. Kubo, *Angew. Chem., Int. Ed.*, 2018, **57**, 16516−16519.
3. L. Ren and N. Jiao, *Chem. – Asian J.*, 2014, **9**, 2411−2414.
4. G. Sheldrick, *Acta Cryst. A*, 2015, **71**, 3−8.
5. G. Sheldrick, *Acta Cryst. C*, 2015, **71**, 3−8.
6. O. V. Dolomanov, L. J. Bourhis, R. J. Gildea, J. A. K. Howard and H. Puschmann, *J. Appl. Cryst.*, 2009, **42**, 339−341.
7. Gaussian 09, Revision A.1. M. J. Frisch, G. W. Trucks, H. B. Schlegel, G. E. Scuseria, M. A. Robb, J. R. Cheeseman, G. Scalmani, V. Barone, B. Mennucci, G. A. Petersson, H. Nakatsuji, M. Caricato, X. Li, H. P. Hratchian, A. F. Izmaylov, J. Bloino, G. Zheng, J. L. Sonnenberg, M. Hada, M. Ehara, K. Toyota, R. Fukuda, J. Hasegawa, M. Ishida, T. Nakajima, Y. Honda, O. Kitao, H. Nakai, T. Vreven, J. A. Montgomery, Jr., J. E. Peralta, F. Ogliaro, M. Bearpark, J. J. Heyd, E. Brothers, K. N. Kudin, V. N. Staroverov, T. Keith, R. Kobayashi, J. Normand, K. Raghavachari, A. Rendell, J. C. Burant, S. S. Iyengar, J. Tomasi, M. Cossi, N. Rega, J. M. Millam, M. Klene, J. E. Knox, J. B. Cross, V. Bakken, C. Adamo, J. Jaramillo, R. Gomperts, R. E. Stratmann, O. Yazyev, A. J. Austin, R. Cammi, C. Pomelli, J. W. Ochterski, R. L. Martin, K. Morokuma, V. G. Zakrzewski, G. A. Voth, P. Salvador, J. J. Dannenberg, S. Dapprich, A. D. Daniels, O. Farkas, J. B. Foresman, J. V.Ortiz, J. Cioslowski, and D. J. Fox, Gaussian, Inc.,

Wallingford CT, 2009.
8. Y. Zhao and D. G. Truhlar, *Theor. Chem. Account.*, 2008, **120**, 215−241.
9. A. D. Becke, *J. Chem. Phys.*, 1993, **98**, 5648−5652.
10. C. Lee, W. Yang, R. G. Parr, *Phys. Rev. B: Condens. Matter Mater. Phys.*, 1988, **37**, 785−789.
11. T. Yanai, D. P. Tew and N. C. Handy, *Chem. Phys. Lett.*, 2004, **393**, 51−57.
12. R. Ditchfield, W. J. Hehre and J. A. Pople, *J. Chem. Phys.*, 1971, **54**, 724−728.
13. W. J. Hehre, R. Ditchfield and J. A. Pople, *J. Chem. Phys.*, 1972, **56**, 2257−2261.
14. P. C.Hariharan, J. A. Pople, *Theor. Chim. Acta*, 1973, **28**, 213−222.